Enhanced Fast Handover for Network Mobility in Intelligent Transportation Systems

Seonggeun Ryu, Kyung-Joon Park, *Member, IEEE*, and Ji-Woong Choi, *Senior Member, IEEE*

***Abstract*—To maintain the Internet connectivity of a group of nodes in intelligent transportation systems (ITSs), the network mobility basic support (NEMO BS) protocol was standardized. The NEMO BS provides mobility for mobile network nodes (MNNs) in a moving network through a mobile router (MR). Since packet loss in NEMO dramatically increases during a handover as the number of MNNs increases, Mobile IPv6 fast handovers (FMIPv6) was adopted to reduce packet loss and handover latency. However, since FMIPv6 was originally designed for a single mobile node (MN), FMIPv6 based on NEMO (fNEMO) incurs a high tunneling burden on the link between the previous and new access routers (PAR and NAR, respectively). In this paper, we propose an *enhanced fNEMO (EfNEMO)* as an efficient fast handover scheme that significantly mitigates the tunneling burden and handover latency. In particular, EfNEMO performs a tentative binding update (BU) procedure to register a new care-of address (NCoA) for the MR with the MR's home agent (HA) before the layer-2 handover. Consequently, EfNEMO delivers packets destined for MNNs via various paths between the HA and the NAR without any tunneling. Furthermore, EfNEMO reduces handover latency because it performs the registration to the HA in advance. By establishing an analytical model for the proposed EfNEMO, we investigate the handover performance of NEMO, fNEMO, and EfNEMO. In addition, we compare EfNEMO with NEMO and fNEMO in terms of the overall cost and the handover latency. Simulation is also performed to compare in a more realistic environment. The results of analysis and simulation show that EfNEMO significantly outperforms fNEMO and NEMO.**

***Index Terms*—Fast handover (FMIPv6), Mobile IPv6 intelligent transportation systems (ITS), mobility management, network mobility (NEMO), performance analysis.**

I. Introduction

RECENTLY, there has been significant interest and progress in the field of intelligent transportation systems (ITSs) from both industry and academia. The main contribution of ITSs is to significantly increase road safety. However, the role of infotainment has rapidly taken an important place [1]. The new emerging infotainment applications or safety-related mobile applications call for vehicular communication networks to support seamless wireless Internet services in fast-moving vehicles [2]. Internet access in automotive scenarios is a particularly relevant case, particularly because people in modern cities spend much time in transportation and vehicles. Public transportation systems, such as subways, suburb trains, and city buses, represent one relevant scenario because of a group of users and the time spent by these users in transportation and vehicles [3]. To maintain a vehicle's Internet connectivity for a group of nodes that are moving together, network mobility basic support (NEMO BS) [4] was developed by the Internet Engineering Task Force. NEMO BS is considered in ITS standards because it is a protocol that is able to provide network mobility [5]. NEMO BS, a mobility support protocol specially designed to manage mobility of a moving network, ensures session continuity for all the nodes in a mobile network [4]. In NEMO, a special device called a mobile router (MR) is defined to extend the mobile node (MN) of mobile IPv6 (MIPv6) [6] by adding capability routing between its point of attachment and a subnet that moves with the MR. The International Organization for Standardization (ISO) TC204 WG16 has developed Communications Access for Land Mobiles (CALM), which adopts NEMO BS referred to as the ITS station reference architecture [7]. The European Telecommunications Standards Institute (ETSI) has standardized geographic addressing and routing (GeoNetworking) initially specified by the GeoNet European project [8], and NEMO BS has been combined with GeoNetworking [9], [10].

Although NEMO BS seems to fit well in the context of ITSs by providing connectivity for mobile network nodes (MNNs) attached to the MR, it has several problems. One of the problems is that packet loss and long handover latency during the handover were inherited from MIPv6. This issue is more critical in NEMO as MNNs in a mobile network move at the same time. Several studies have attempted to solve these problems [11]–[16]. The main idea behind these solutions is to incorporate a fast handover scheme (FMIPv6) [17] with NEMO BS. This is because FMIPv6 reduces packet loss by using tunneling and buffering, and it shortens the handover latency by performing several parts of the handover process in advance. In this paper, we call these solutions fNEMO and focus on enhancing fNEMO. The other problem of NEMO is that NEMO BS does not incorporate route optimization (RO) by which MNNs can directly communicate with correspondent nodes (CNs). There have been many proposals to carry out RO in various NEMO environments [18]–[24]. These proposals enable MNNs to communicate with their CNs directly in various scenarios. In this paper, we do not consider RO for NEMO.

Manuscript received May 1, 2012; revised October 9, 2012, January 13, 2013, and April 25, 2013; accepted June 6, 2013. Date of publication July 3, 2013; date of current version January 13, 2014. This work was supported in part by the National Research Foundation of Korea under Grant 2010-0022076 and Grant 2012R1A1A1009742 and in part by the Daegu Gyeongbuk Institute of Science and Technology through their Research and Development Program under Grant 13-DB-04. The review of this paper was coordinated by Prof. Y.-B. Lin. *(Corresponding author: J.-W. Choi.)*

S. Ryu was with the Department of Information and Communication Engineering, Daegu Gyeongbuk Institute of Science and Technology, Daegu 711-873, Korea. He is now with LG Electronics, Seoul 137-130, Korea (e-mail: sunggooni@gmail.com).

K.-J. Park and J.-W. Choi are with the Department of Information and Communication Engineering, Daegu Gyeongbuk Institute of Science and Technology, Daegu 711-873, Korea (e-mail: kjp@dgist.ac.kr; jwchoi@dgist.ac.kr).

Digital Object Identifier 10.1109/TVT.2013.2272059

Since fNEMO combines NEMO BS with FMIPv6 without considering the properties of NEMO where many MMNs move at the same time, it is not suitable for NEMO. In fNEMO, a tunnel between a previous access router (PAR) and a new access router (NAR) may be occasionally overloaded with traffic destined for MNNs. This is because the tunnel established in fNEMO is for just one MN as in FMIPv6. For example, if there are many MNNs, the traffic of the MNNs converges in the tunnel, which then may become overloaded. In particular, if the traffic density of MNNs is high, the tunnel is more overloaded and may suffer from congestion. Thus, the tunneling burden may incur packet loss during the handover.

In this paper, we propose a scheme for enhancing fNEMO (EfNEMO), which eliminates the tunneling burden of fNEMO. EfNEMO adopts the tentative binding update (BU) scheme proposed in [25] and [26] to early register a new care-of address (NCoA) with the MR's home agent (HA). Then, packets destined for MNNs are delivered not via the tunnel between the PAR and the NAR but via various paths between the HA and the NAR. Thus, tunneling is not used in EfNEMO. The handover latency is reduced as well because the registration to the HA is performed in advance.

Accordingly, the main contributions of this paper are given as follows. First, we propose an enhanced fast handover scheme (EfNEMO), which is an effective scheme for NEMO in ITSs. We first point out the significant tunneling burden of fNEMO, which has not been properly elucidated in previous studies, whereas EfNEMO eliminates that tunneling burden. Second, in addition to mitigating the tunneling burden, EfNEMO further reduces the handover latency. EfNEMO performs a registration process of the NCoA during the layer-2 handover, whereas fNEMO carries it out after the layer-2 handover. Thus, EfNEMO achieves a smaller handover latency than fNEMO. Third, we develop an analytical model for EfNEMO to compare NEMO, fNEMO, and EfNEMO. In the performance analysis, we consider the cost of tunneling and buffering to investigate the handover performance as important parameters. We also analyze both the predictive and reactive modes of FMIPv6 altogether. In addition, we provide simulation results to validate our models. Through simulation results, we can provide a more realistic comparison between fNEMO and EfNEMO. Fourth, EfNEMO requires only minor modifications to fNEMO. Hence, if the PAR, the NAR, or the HA is not aware of EfNEMO, fNEMO will operate without a further process.

The rest of this paper is organized as follows. Section II describes NEMO BS and fNEMO. In Section III, we describe the proposed scheme, an enhanced fast handover scheme based on NEMO (EfNEMO). In Sections IV and V, performance analysis and numerical results are presented, respectively. Finally, our conclusion follows in Section VI.

II. Background

Here, we describe the concepts and protocols of network mobility management, NEMO BS, and the integration of FMIPv6 with NEMO BS, i.e., fNEMO. Here, we mainly describe the handover operation, whereas the handover latency is explained in the performance analysis.

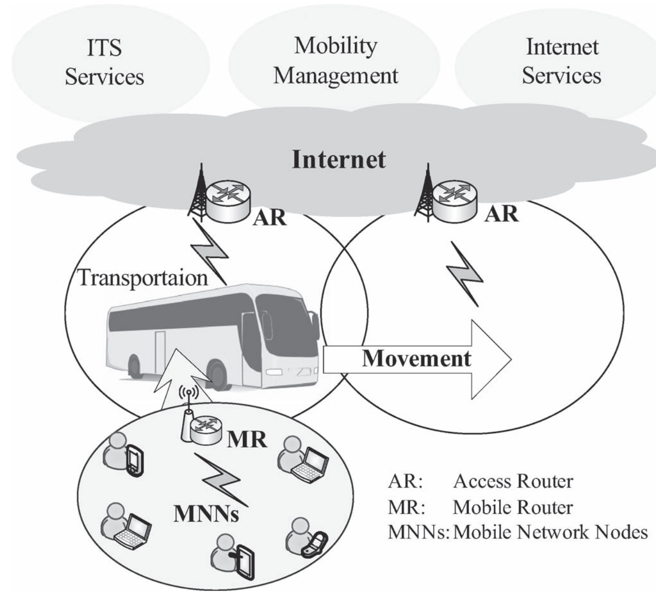

Fig. 1. Architecture overview of NEMO.

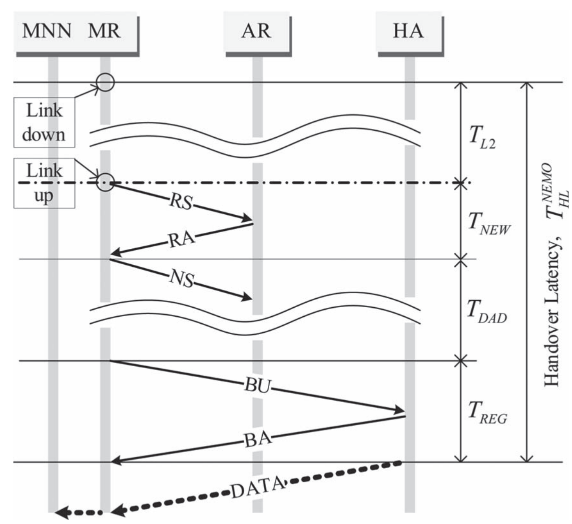

Fig. 2. Handover operation and timing diagram in NEMO.

A. NEMO BS Protocol

To support ITS applications, Internet access is required in the vehicle. For example, fixed vehicle sensors, passengers' mobile devices, or even a personal area network (PAN) moving with a vehicular network may connect to the Internet. In this scenario, to reduce the signaling burden of each node in the vehicle, NEMO BS, which supports network mobility in the vehicular networks, was introduced. NEMO BS is an efficient and scalable scheme because the mobility management is transparent to each node in the vehicle. That is, MNNs, which are nodes connected to an MR, do not send and receive signaling messages during the handover. Fig. 1 shows an architecture overview of NEMO. The objective of NEMO BS is to maintain session continuity between the MNNs and the CNs, whereas the MR changes its point of attachment. Fig. 2 shows the handover operation and timing diagram in NEMO. The handover that we consider here consists of the layer-2 handover and the layer-3

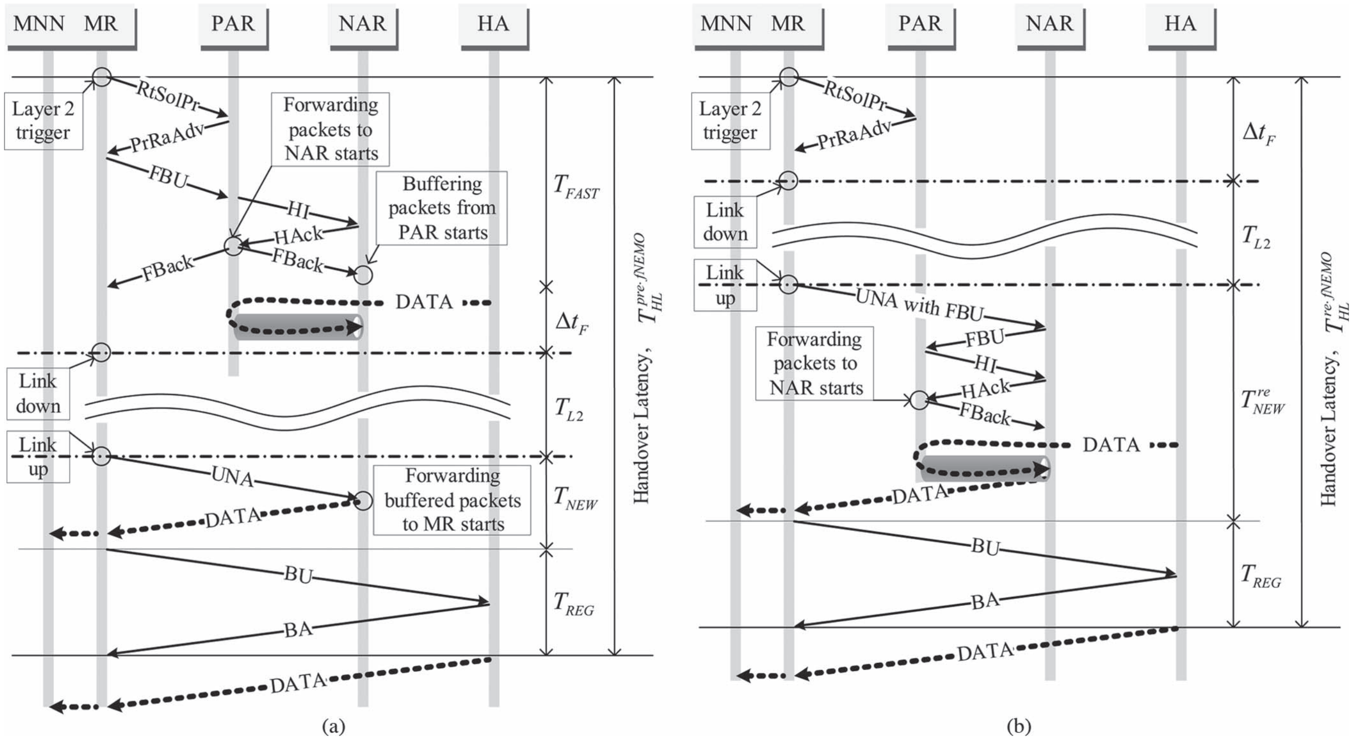

Fig. 3. Handover operations and timing diagrams in fNEMO. (a) Predictive mode of fNEMO. (b) Reactive mode of fNEMO.

handover. The layer-2 handover is to switch the link of the previous access point (AP) to that of a new AP. As shown in Fig. 2, it is processed during the period between the downlink and uplink. Briefly, the layer-3 handover is composed of movement detection (MD), address autoconfiguration, and registration. For example, when the MR moves between networks, after the link switching, it must detect the movement, configure a NCoA, and register the NCoA with its HA.

NEMO BS is initiated when the MR attaches to a new AR. The handover operation of NEMO BS is the same as that of MIPv6, except that MNNs do not participate in this operation. To obtain information on the new network, router solicitation (RS) and router advertisement (RA) messages are exchanged between the MR and the AR. Then, the MR creates an NCoA and performs a duplicate address detection (DAD) [27] procedure using a neighbor solicitation (NS) message to verify the uniqueness of the addresses on the link. As soon as the NCoA is verified, the MR sends a BU message to the HA to register the NCoA. On receiving the BU message, the HA creates a cache entry binding the MR's home address (HoA) to the NCoA. When the MR receives the affirmative binding acknowledgement (BA) message from the HA, the handover operation is completed. Thus, MNNs can communicate with CNs via the HA.

B. fNEMO

NEMO BS inherits the problems of MIPv6 because it is based on MIPv6. The representative problems are packet loss and long handover latency. Thus, schemes that incorporate NEMO BS with FMIPv6 (fNEMO) have been proposed [11]–[16] because FMIPv6 can reduce packet loss and long handover latency. The main idea behind fNEMO is to perform several parts of the handover process in advance. Furthermore, a tunnel between the PAR and the NAR is established in this process. Packets destined for MNNs are delivered via the tunnel and are then buffered in the NAR during the handover. Hence, fNEMO can prevent packet loss and reduce the handover latency.

The handover operation of fNEMO is the same as that of FMIPv6, except that the MR participates in the handover on behalf of MNNs. The handover operations and timing diagrams in fNEMO are shown in Fig. 3. The operation of fNEMO is divided into two modes, the predictive mode and the reactive mode, as in FMIPv6. These two operations are determined according to whether a fast BA (FBack) message is received on the previous link during the handover. The handover of the predictive mode is initiated when a layer-2 trigger occurs. The MR sends an RS for proxy advertisement (RtSolPr) message to the PAR to obtain information about neighboring links facilitating MD. With the information provided in a proxy RA (PrRtAdv) message, which is a response to the RtSolPr message, the MR creates an NCoA and sends a fast BU (FBU) message to the PAR. The purpose of the FBU message is to bind the previous CoA to the NCoA so that packets arriving at the PAR can be tunneled to the new location of the MR. Then, the PAR and the NAR exchange a handover initiate (HI) and handover acknowledge (HAck) messages to transfer network-resident contexts. At that time, a tunnel between the PAR and the NAR is established. On receiving the HAck message, the PAR starts to forward packets destined for the MR to the NAR and sends the FBack messages to the MR and the NAR. The NAR then starts to buffer packets delivered via the tunnel. As soon as the layer-2 handover is finished, the MR sends an unsolicited neighbor advertisement (UNA) message to the NAR to inform the NAR of the attachment. On receiving the UNA message, the NAR starts to forward buffered packets to the MR.

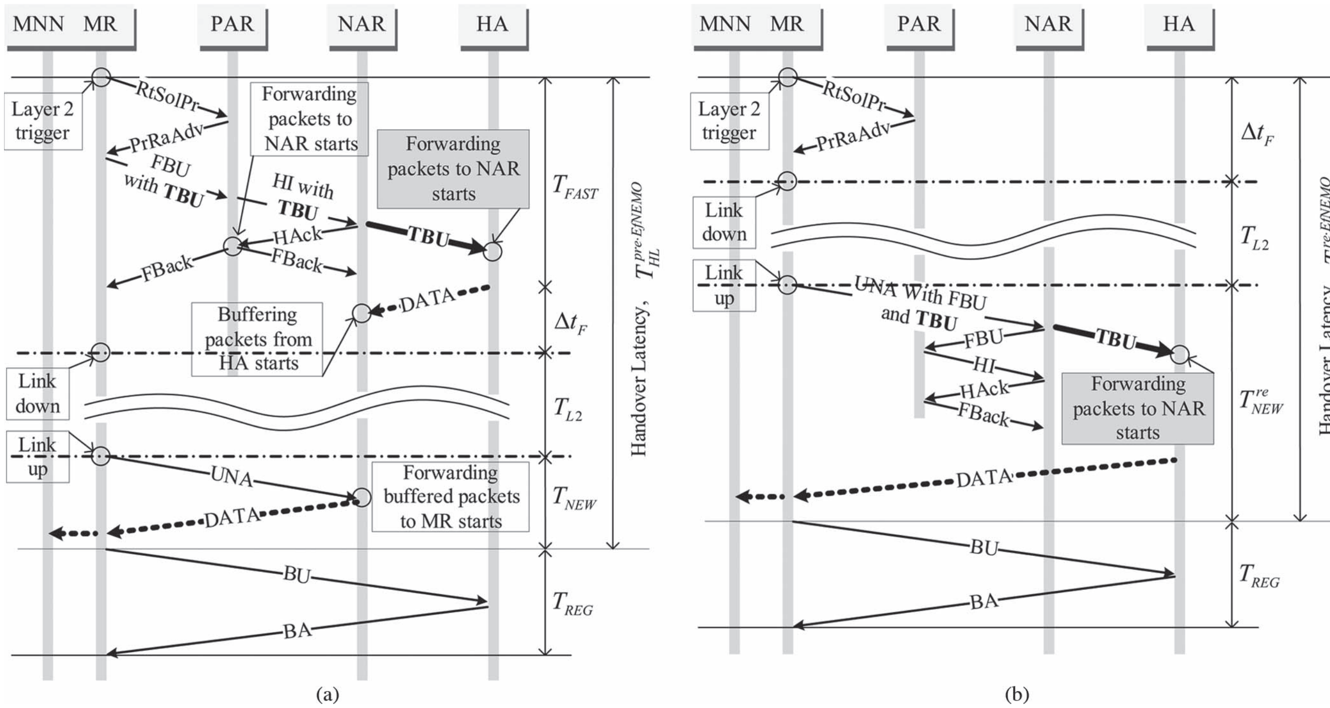

Fig. 4. Handover operations and timing diagrams in EfNEMO. (a) Predictive mode of EfNEMO. (b) Reactive mode of EfNEMO.

Finally, the MR registers the NCoA with its HA through the BU and BA messages.

If the MR does not receive the FBack message before the layer-2 handover, fNEMO operates in the reactive mode. In the reactive mode of fNEMO, the MR sends the UNA message, including the FBU message, to the NAR after the layer-2 handover is finished. The NAR forwards the FBU message to the PAR, and then HI and HAck messages are exchanged between the PAR and the NAR. As a result, a tunnel between the PAR and the NAR is established. On receiving the HAck message, the PAR starts to forward packets and sends the FBack message to the NAR. Before registering the NCoA, packets are delivered to the MR via the tunnel.

III. Enhanced Fast Handover for Network Mobility

In the previous studies, fNEMO was investigated by incorporating FMIPv6 with NEMO BS. However, in fNEMO, the characteristics of NEMO were not fully examined. For example, many MNNs connected to the MR in NEMO move at the same time, which may cause serious performance degradation during the handover. Since FMIPv6 is designed for a single MN, a tunnel between the PAR and the NAR, which is established during the handover, is used for the single MN. On the other hand, in fNEMO, packets destined for every MNN are delivered via the tunnel. As the number of MNNs increases, the burden on the tunnel increases. When many MNNs send or receive with high traffic density, the tunnel is particularly overloaded, which results in serious congestion.

Our key idea is to mitigate the burden on the tunnel and to reduce the handover latency. In a nutshell, we propose EfNEMO to perform registration to the HA in advance to enhance the handover performance of fNEMO. When several parts of the handover process are performed, a tentative registration is also performed. As a result, traffic to MNNs is delivered via paths between the HA and the NAR and not via the tunnel between the PAR and the NAR during the handover. EfNEMO eliminates the burden on the tunnel between the PAR and the NAR, and reduces the impact of any possible failure of the tunnel. In addition, the handover latency is reduced because the registration to the HA is already performed. Therefore, EfNEMO may be a suitable solution for NEMO in ITS.

Fig. 4 shows the detailed handover operation and timing sequences in EfNEMO. The operation of EfNEMO is divided into the predictive mode and the reactive mode because EfNEMO is based on fNEMO. Message flows of EfNEMO follow those of fNEMO, except sending a tentative BU (TBU) message. When the MR creates the FBU message, it also creates the TBU message, and then the TBU message is embedded in the FBU message. The TBU message is a TBU message that registers the NCoA in advance. The TBU message is delivered to the HA via the FBU and the HI messages. On receiving the TBU message, the HA tentatively creates an additional entry in a binding cache entry (BCE) using binding information. Thus, two bindings concerning the MR's HoA coexist in the BCE during the handover. This is because the HA has to forward packets to the PAR when the MR does not move to the NAR after sending the TBU message to avoid the ping-pong effect. The binding information on the TBU message consists of the MR's HoA, the NCoA, and the short binding lifetime. Then, the HA starts to forward packets to the NAR, and packets are buffered in the NAR. As a result, the tunnel between the PAR and the NAR is not used in EfNEMO. Thus, packets destined for MNNs are delivered to the NAR via various paths between the HA and the NAR during the handover. In

TABLE I
NOTATIONS

Notation	Description	Notation	Description
D_h	Horizontal dimension of analysis area	D_v	Vertical dimension of analysis area
N_h	The number of horizontal roads	N_v	The number of vertical roads
S_h	Horizontal road distance	S_v	Vertical road distance
m	The number of APs in each row	n	The number of AP rows
T_r	The average residence time in an AP	U_{max}	Maximum random pause time
r	The radius of a cell	v	average speed of vehicles
μ_h	The average handover rate	p_{pmf}	The probability of predictive mode failure
θ_1	The adjustment factor for the vehicle in μ_h	θ_2	The adjustment factor for the vehicle p_{pmf}
n_f	The number of link failures	$t_d(L)$	The wired link delay with L length of a packet
$E[n_f]$	The mean number of n_f	$t_l(L)$	The wireless link delay with L length of a packet
T_{wl}	Wireless propagation delay	T_{wd}	Wired propagation delay
B_{wl}	The bandwidth of wireless link	B_{wd}	The bandwidth of wired link
T_{L2}	The link switching delay	T_p	The processing time
p_{wlf}	The probability of wireless link failure	ω	A weight factor for wireless link
ϵ	A weight factor for the packet loss cost	n_{MNN}	The number of MNNs
λ_p	Packet arrival rate	τ	A weight factor for tunneling
β	A weight factor for buffering	L_X	The length of the X message
d_{Y-Z}	The distance between Y and Z nodes		

EfNEMO, the tunnel between the PAR and the NAR remains, so that the tunnel is used when the HA cannot process the TBU message, or the TBU message is not delivered. After the layer-2 handover is finished, the MR registers the NCoA with its HA to update the BCE regarding its HoA through a regular BU message.

In the reactive mode of EfNEMO, the TBU message is embedded in the UNA message and is forwarded to the HA. The rest of the operation is similar to the reactive mode of fNEMO. In the reactive mode of EfNEMO, the tunnel between the PAR and the NAR can be used when the TBU scheme is not performed in the predictive mode of EfNEMO.

IV. Performance Analysis

Here, we develop analytical models to investigate the handover performances of EfNEMO compared with NEMO and fNEMO. The performances of EfNEMO, fNEMO, and NEMO are compared in terms of the overall cost and the handover latency. Notations used in the performance analysis are listed in Table I.

A. Analytical Models

We use the city section mobility (CSM) model introduced in [28] and [29]. The CSM model represents a movement behavior that is influenced by constraints of the environment. In real-life scenarios, vehicles do not have the ability to travel freely since they have to follow traffic regulations. The CSM model is a realistic movement pattern for vehicles in a city [30], and its stochastic properties have been analyzed in [31]. Thus, we adopt those properties for our mobility model.

The area used in CSM model for analysis is represented by a grid of streets forming a particular section of a city. The model sets parameters, such as the speed limit of each street. An MR starts at a predefined intersection of two streets, and then it randomly chooses a destination. When the MR reaches the destination, it pauses for a random time and then chooses another destination randomly, and the process is repeated. Each cycle is termed an epoch [31].

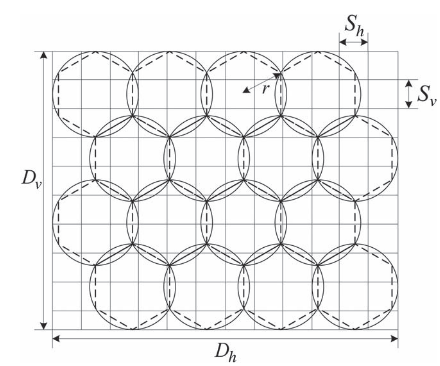

Fig. 5. Road network in the CSM model.

Let the environment be a rectangular area of dimension $D_h \times D_v$, as shown in Fig. 5, where roads are parallel to axes. N_h and N_v are the numbers of horizontal and vertical roads, respectively. Horizontal roads are S_h distance apart, and vertical roads are S_v distance apart. Then, $N_h = D_h/S_h + 1$ and $N_v = D_v/S_v + 1$. Therefore, the expected epoch length is obtained as follows [31]:

$$E(L) = \frac{D_h \cdot (N_h + 1)}{3N_h} + \frac{D_v \cdot (N_v + 1)}{3N_v}.$$

Let v be an average velocity of a vehicle. Then, the expected epoch time is calculated as

$$E(T) = \frac{E(L)}{v}. \quad (1)$$

For safety at each road intersection, there is a random pause time between 0 to $U_{\max}$ to avoid collisions. Hence, the expected pause time can be represented by

$$E(P) = \frac{U_{\max}}{2}. \quad (2)$$

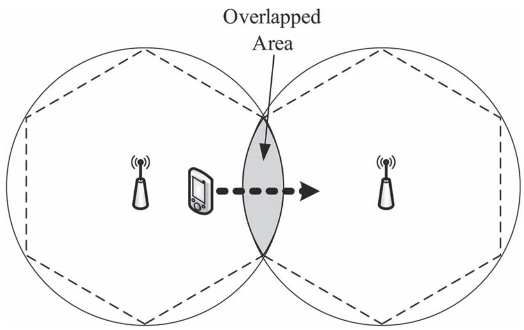

Fig. 6. Overlapping area between boundary cells.

In Fig. 5, APs cover the road network of dimensions $D_h \times D_v$. There are n rows of APs and m APs in each row, so that $m \cdot n$ APs cover the rectangular area. Let the radio coverage area of each AP be a circular region of radius r and two successive APs overlap at lengths of l_h and l_v along their horizontal and vertical diameters, respectively. Then, $D_h = 2r \cdot m - (m-1) \cdot l_h$, $D_v = 2r \cdot n - (n-1) \cdot l_v$, $l_h = (2-\sqrt{3}) \cdot r$, and $l_v = r/2$. Therefore, m and n are given by

$$m = \left\lceil \frac{D_h - 2 \cdot r + \sqrt{3} \cdot r}{\sqrt{3} \cdot r} \right\rceil$$

$$n = \frac{2b - r}{3r}.$$

We assume that $2r = K_1 \cdot S_h = K_2 \cdot S_v$. The expected number of APs crossing in an epoch can be obtained as [30] and [31]

$$E(C) = \frac{m \cdot (m+1) \cdot K_1}{6N_h^2} \cdot (6N_h - 4m \cdot K_1 + K_1 + 3) + \frac{n \cdot (n+1) \cdot K_2}{6N_v^2} \cdot (6N_v - 4n \cdot K_2 + K_2 + 3). \quad (3)$$

Finally, using (1), (2), and (3), the average residence time in an AP is estimated as [31]

$$T_r = \frac{E(T) + E(P)/3600}{E(C)} \times 3600. \quad (4)$$

Since we assume that an AR's area is equal to an AP's area, we can obtain the handover rate μ_h by using (4) as follows:

$$\mu_h = \frac{1}{T_r}.$$

In fast handover schemes based on FMIPv6, such as fNEMO and EfNEMO, additional signaling messages may be exchanged between an MR and a PAR, whereas the MR is in the overlapping area between the PAR and the NAR. The predictive mode will fail when the MR leaves the overlapping area before transmission of the additional signaling messages can be completed. If the predictive mode fails, the reactive mode is activated. Then, the probability of the predictive mode failure p_{pmf} has to be given to evaluate the performances of fNEMO and EfNEMO. Fig. 6 shows the overlapping area of boundary cells. Let T be a random variable for the time from the layer-2 trigger epoch to the downlink, i.e., pending a layer-2 handover. Then, p_{pmf} can be represented by [32]

$$p_{\text{pmf}} = \Pr(T < T_{\text{FAST}}) = \int_0^{T_{\text{FAST}}} f_T(t)dt, \quad T \geq 0$$

where T_{FAST} is the required time for additional signaling in fNEMO or EfNEMO before the layer-2 handover. If we assume that T is exponentially distributed [33], $f_T(t) = \lambda \cdot e^{-\lambda \cdot t}$. Therefore, p_{pmf} is given by

$$p_{\text{pmf}} = 1 - e^{-\lambda \cdot T_{\text{FAST}}}$$

where λ is the arrival rate of the MR into the overlapping area. Using the average residence time T_r, λ can be obtained as

$$\lambda = \frac{1}{T_r \cdot R_O \times 1000}$$

where R_O is the overlapping area rate of a cell area. The overlapping area is $((2\pi - 3\sqrt{3}) \cdot r^2)/12$, and a cell area is $\pi \cdot r^2$; thus, $R_O = (2\pi - 3\sqrt{3})/12\pi$.

B. Analysis of the Handover Latency

We define the handover latency as the time interval between the moment that the layer-2 trigger is initiated and the moment that the MNNs directly receive the first packets from the CNs in the new network. The handover latency consists of layer-2 and layer-3 latencies, such as link switching, MD, address configuration, and registration. The handover latencies of NEMO, fNEMO, and EfNEMO are calculated as in Figs. 2, 3, and 4, respectively.

In Fig. 2, the handover latency of NEMO $T_{\text{HL}}^{\text{NEMO}}$ is calculated as follows:

$$T_{\text{HL}}^{\text{NEMO}} = T_{\text{L2}} + T_{\text{MD}} + T_{\text{DAD}} + T_{\text{REG}}$$

where T_{L2} is the link switching delay, T_{MD} is the delay for performing MD, T_{DAD} is the delay for performing DAD after configuring an NCoA, and T_{REG} is the delay for registering the NCoA with the HA.

In fNEMO and EfNEMO, the handover latencies are divided into those of the predictive mode and the reactive mode, respectively. Then, the handover latencies of fNEMO $T_{\text{HL}}^{\text{fN}}$ and that of EfNEMO $T_{\text{HL}}^{\text{EfN}}$ are obtained as follows:

$$T_{\text{HL}}^{\text{fN}} = (1 - p_{\text{pmf}}) \cdot T_{\text{HL}}^{p \cdot \text{fN}} + p_{\text{pmf}} \cdot T_{\text{HL}}^{r \cdot \text{fN}}$$
$$T_{\text{HL}}^{\text{EfN}} = (1 - p_{\text{pmf}}) \cdot T_{\text{HL}}^{p \cdot \text{EfN}} + p_{\text{pmf}} \cdot T_{\text{HL}}^{r \cdot \text{EfN}}$$

where $T_{\text{HL}}^{p \cdot \text{fN}}$, $T_{\text{HL}}^{r \cdot \text{fN}}$, $T_{\text{HL}}^{p \cdot \text{EfN}}$, and $T_{\text{HL}}^{r \cdot \text{EfN}}$ are the handover latencies of the predictive mode and the reactive mode of fNEMO and EfNEMO, respectively. Then, referring to Fig. 3, $T_{\text{HL}}^{p \cdot \text{fN}}$ and $T_{\text{HL}}^{r \cdot \text{fN}}$ are expressed as follows:

$$T_{\text{HL}}^{p \cdot \text{fN}} = T_{\text{FAST}} + \Delta t_F + T_{\text{L2}} + T_{\text{NEW}} + T_{\text{REG}}$$
$$T_{\text{HL}}^{r \cdot \text{fN}} = \Delta t_F + T_{\text{L2}} + T_{\text{NEW}}^{\text{re}} + T_{\text{REG}}$$

where Δt_F is the time elapsed from the reception of the FBack message on the previous link to the beginning of the layer-2 handover [34], $T_{\rm NEW}$ is the delay for informing the NAR of the attachment in the predictive mode of the fast handover scheme, and $T_{\rm NEW}^{\rm re}$ is the delay for establishing the tunnel between the PAR and the NAR in the reactive mode. In EfNEMO, registration is performed in advance, so that $T_{\rm REG}$ can be eliminated from the handover latency. Then, referring to Fig. 4, $T_{\rm HL}^{p\cdot{\rm EfN}}$ and $T_{\rm HL}^{r\cdot{\rm EfN}}$ are calculated as follows:

$$T_{\rm HL}^{p\cdot{\rm EfN}} = T_{\rm FAST} + \Delta t_F + T_{\rm L2} + T_{\rm NEW}$$

$$T_{\rm HL}^{r\cdot{\rm EfN}} = \Delta t_F + T_{\rm L2} + T_{\rm NEW}^{\rm re}.$$

To calculate each delay consisting of the handover latency, delays on wired and wireless links are obtained by summing the transmission delay, the propagation delay, and the processing delay. The delay for one hop wired link with L length of a packet $t_d(L)$ is given by

$$t_d(L) = \frac{L}{B_{\rm wd}} + T_{\rm wd} + \varpi_q \qquad (5)$$

where $B_{\rm wd}$ is the bandwidth of the wired link, $T_{\rm wd}$ is the propagation delay on the wired link, and ϖ_q is the average queueing delay at each router in the Internet. In the case of the wireless link delay, wireless link failure is considered. Let n_f and P_{n_f} be the number of wireless link failures and the probability that a message transmission over the wireless link fails n_f times before the message is successfully transmitted [35]. The mean number of n_f, i.e., $E[n_f]$, is expressed as follows [35]:

$$E[n_f] = \sum_{n_f=0}^{\infty} n_f \cdot P_{n_f} = \frac{p_{\rm wlf}}{1-p_{\rm wlf}}$$

where $p_{\rm wlf}$ is the probability of wireless link failure. Thus, the wireless link delay $t_w(L)$ is calculated as follows:

$$t_w(L) = \left(\frac{L}{B_{\rm wl}} + T_{\rm wl} + T_p\right) + E[n_f]\cdot\left(\frac{L}{B_{\rm wl}} + T_{\rm wl} + T_p + T_{\rm wait}\right) \qquad (6)$$

where $T_{\rm wait}$ is the waiting time to determine that the message was lost, $B_{\rm wl}$ is the bandwidth of the wireless link, $T_{\rm wl}$ is the propagation delay on the wireless link, and T_p is the processing time. Let $T_{\rm wait} = \eta \cdot ((L/B_{\rm wl}) + T_{\rm wl} + T_p)$ because the waiting time may be determined by the round trip time, where η is a weight factor for the waiting time. Then, (6) becomes

$$t_w(L) = \left(\frac{1+\eta\cdot p_{\rm wlf}}{1-p_{\rm wlf}}\right)\cdot\left(\frac{L}{B_{\rm wl}} + T_{\rm wl} + T_p\right). \qquad (7)$$

Using (5) and (7), $T_{\rm MD}$, $T_{\rm NEW}$, $T_{\rm NEW}^{\rm re}$, $T_{\rm FAST}$, and $T_{\rm REG}$ are expressed as follows:

$$\begin{aligned}
T_{\rm MD} &= t_w(L_{\rm RS}) + t_w(L_{\rm RA})\\
T_{\rm NEW} &= t_w(L_{\rm UNA}) + t_w(L_{\rm DATA})\\
T_{\rm NEW}^{\rm re} &= t_w(L_{\rm UNA} + L_{\rm FBU} + L_{\rm TBU}) + t_w(L_{\rm DATA})\\
&\quad + d_{\rm AR-AR}\cdot(t_d(L_{\rm FBU}) + t_d(L_{\rm HI})\\
&\quad + t_d(L_{\rm HAck}) + t_d(L_{\rm FBack}))\\
T_{\rm FAST} &= t_w(L_{\rm RS}) + t_w(L_{\rm RA}) + t_w(L_{\rm FBU})\\
&\quad + d_{\rm AR-AR}\cdot(t_d(L_{\rm HI}) + t_d(L_{\rm HAck}))\\
&\quad + \max\left(t_w(L_{\rm FBack})t_d(L_{\rm FBack})\right)\\
T_{\rm REG} &= t_w(L_{\rm BU}) + d_{\rm HA-AR}\cdot(t_d(L_{\rm BU}) + t_d(L_{\rm BA}))\\
&\quad + t_w(L_{\rm BA})
\end{aligned}$$

where L_X is the length of the X message, and $d_{\rm AR-AR}$ and $d_{\rm HA-AR}$ are hop distances between the ARs and between the HA and the AR, respectively.

C. Analysis of the Overall Cost

Here, we derive the cost function of the signaling overhead and the packet delivery cost to investigate NEMO, fNEMO, and EfNEMO. The signaling overhead is defined as the mobility signaling overhead incurred during the handover, and it is calculated by the product of the message length and the hop distance [21]. The packet delivery cost is introduced to analyze additionally transmitted data packets due to duplicate delivery, tunneling, buffering, and packet loss during the handover. A duplicate delivery cost is incurred when the PAR forwards packets to both the NAR and the MR, simultaneously. A tunneling cost is incurred when the tunnel between the PAR and the NAR is used to forward packets. A buffering cost is incurred when the NAR buffers the packets destined for the MR before the MR connects to the NAR. A packet loss cost is incurred when packets are not prevented through tunneling and buffering during the handover. Each cost is calculated as the product of the data packet size, the hop distance, and the elapsed time.

The signaling overhead of NEMO, $C_{\rm SOH}^{\rm NEMO}$ is expressed as follows:

$$C_{\rm SOH}^{\rm NEMO} = \mu_h\cdot(S_{\rm MD} + S_{\rm DAD} + S_{\rm REG})$$

where $S_{\rm MD}$, $S_{\rm DAD}$, and $S_{\rm REG}$ are the signaling costs caused by the MD process, DAD, and the registration procedure, respectively. Referring to Fig. 2, $S_{\rm MD}$, $S_{\rm DAD}$, and $S_{\rm REG}$ are calculated as follows:

$$\begin{aligned}
S_{\rm MD} &= \omega\cdot(L_{\rm RS} + L_{\rm RA}) + E[n_f]\cdot\omega\cdot(L_{\rm RS} + L_{\rm RA})\\
&= \frac{\omega\cdot(L_{\rm RS} + L_{\rm RA})}{1-p_{\rm wlf}}\\
S_{\rm DAD} &= \omega\cdot L_{\rm NS} + E[n_f]\cdot\omega\cdot L_{\rm NS} = \frac{\omega\cdot L_{\rm NS}}{1-p_{\rm wlf}}\\
S_{\rm REG} &= \omega\cdot(L_{\rm BU} + L_{\rm BA}) + E[n_f]\cdot\omega\cdot(L_{\rm BU} + L_{\rm BA})\\
&\quad + d_{\rm HA-AR}\cdot(L_{\rm BU} + L_{\rm BA})\\
&= \left(\frac{\omega}{1-p_{\rm wlf}} + d_{\rm HA-AR}\right)\cdot(L_{\rm BU} + L_{\rm BA})
\end{aligned}$$

where ω is a weight factor for the wireless link because in general transmission over a wireless link is more expensive than that over a wired link [36]. In addition, each message via the wireless link is summed by $E[n_f]$ times because the wireless link failure is considered.

In NEMO, all packets destined for MNNs are lost during the handover. Then, the packet delivery cost of NEMO $C_{\mathrm{PD}}^{\mathrm{NEMO}}$ is expressed as follows:

$$C_{\mathrm{PD}}^{\mathrm{NEMO}} = \epsilon \cdot C_{\mathrm{loss}}^{\mathrm{NEMO}}$$

where ϵ is a weight factor for the packet loss cost, and $C_{\mathrm{loss}}^{\mathrm{NEMO}}$ is the packet loss cost. In NEMO, packets destined for MNNs are delivered from the CN via the PAR during the handover, and they are not delivered to the MNNs because the connection between the AR and the MR is lost. Therefore, $C_{\mathrm{loss}}^{\mathrm{NEMO}}$ is obtained as follows:

$$C_{\mathrm{loss}}^{\mathrm{NEMO}} = \mu_h \cdot n_{\mathrm{MNN}} \cdot \mathrm{PD}_{\mathrm{CN-AR}}^{\mathrm{previous}} \cdot \left(T_{\mathrm{HL}}^{\mathrm{NEMO}} - \frac{T_{\mathrm{REG}}}{2}\right)$$

where n_{MNN} is the number of MNNs. In NEMO, data packets are delivered through the tunnel between the HA and the MR, and then the packet delivery cost for one MN $\mathrm{PD}_{\mathrm{CN-AR}}^{\mathrm{previous}}$ is given by

$$\mathrm{PD}_{\mathrm{CN-AR}}^{\mathrm{previous}} = \lambda_p \cdot \{d_{\mathrm{CN-HA}} \cdot L_{\mathrm{DATA}} + d_{\mathrm{HA-AR}} \cdot (L_{\mathrm{DATA}} + L_{\mathrm{THD}})\}$$

where λ_p is the packet arrival rate, $d_{\mathrm{CN-HA}}$ is the distance between the CN and the HA, and L_{DATA} and L_{THD} are the lengths of a data packet and a tunnel header, respectively.

In fNEMO, the predictive mode and the reactive mode are considered. Then, the signaling overhead $C_{\mathrm{SOH}}^{\mathrm{fN}}$ and the packet delivery cost $C_{\mathrm{PD}}^{\mathrm{fN}}$ are expressed as follows:

$$C_{\mathrm{SOH}}^{\mathrm{fN}} = (1 - p_{\mathrm{pmf}}) \cdot C_{\mathrm{SOH}}^{p\cdot\mathrm{fN}} + p_{\mathrm{pmf}} \cdot C_{\mathrm{SOH}}^{r\cdot\mathrm{fN}}$$
$$C_{\mathrm{PD}}^{\mathrm{fN}} = (1 - p_{\mathrm{pmf}}) \cdot C_{\mathrm{PD}}^{p\cdot\mathrm{fN}} + p_{\mathrm{pmf}} \cdot C_{\mathrm{PD}}^{r\cdot\mathrm{fN}}$$

where $C_{\mathrm{SOH}}^{p\cdot\mathrm{fN}}$, $C_{\mathrm{SOH}}^{r\cdot\mathrm{fN}}$, $C_{\mathrm{PD}}^{p\cdot\mathrm{fN}}$, and $C_{\mathrm{PD}}^{r\cdot\mathrm{fN}}$ are the signaling overheads and the packet delivery costs for the predictive mode and the reactive mode of fNEMO, respectively. Referring to Fig. 3, $C_{\mathrm{SOH}}^{p\cdot\mathrm{fN}}$ and $C_{\mathrm{SOH}}^{r\cdot\mathrm{fN}}$ are obtained as follows:

$$C_{\mathrm{SOH}}^{p\cdot\mathrm{fN}} = \mu_h \cdot \left(S_{\mathrm{FAST}}^{\mathrm{fN}} + \frac{S_{\mathrm{MD}}}{2} + S_{\mathrm{REG}}\right)$$
$$C_{\mathrm{SOH}}^{r\cdot\mathrm{fN}} = \mu_h \cdot \left(S_{\mathrm{NEW}}^{r\cdot\mathrm{fN}} + S_{\mathrm{REG}}\right)$$

where $S_{\mathrm{FAST}}^{\mathrm{fN}} = (\omega \cdot (L_{\mathrm{RSP}} + L_{\mathrm{PRA}} + L_{\mathrm{FBU}} + L_{\mathrm{FBack}}))/(1 - p_{\mathrm{wlf}}) + d_{\mathrm{AR-AR}} \cdot (L_{\mathrm{HI}} + L_{\mathrm{HAck}} + L_{\mathrm{FBack}})$, and $S_{\mathrm{NEW}}^{r\cdot\mathrm{fN}} = (\omega \cdot (L_{\mathrm{UNA}} + L_{\mathrm{FBU}}))/(1 - p_{\mathrm{wlf}}) + d_{\mathrm{AR-AR}} \cdot (L_{\mathrm{FBU}} + L_{\mathrm{HI}} + L_{\mathrm{HAck}} + L_{\mathrm{FBack}})$.

In the predictive mode of fNEMO, $C_{\mathrm{PD}}^{p\cdot\mathrm{fN}}$ consists of a duplicate cost $C_{\mathrm{PAR}}^{\mathrm{duplicate}}$, a tunneling cost $C_{\mathrm{tunl}}^{p\cdot\mathrm{fN}}$, and a buffering cost $C_{\mathrm{buff}}^{p\cdot\mathrm{fN}}$, and is expressed as follows:

$$C_{\mathrm{PD}}^{p\cdot\mathrm{fN}} = C_{\mathrm{PAR}}^{\mathrm{duplicate}} + \tau \cdot C_{\mathrm{tunl}}^{p\cdot\mathrm{fN}} + \beta \cdot C_{\mathrm{buff}}^{p\cdot\mathrm{fN}}$$

where τ and β are weight factors of tunneling and buffering, respectively. When the PAR receives the HAck message, it forwards the packets to the MNNs and to the NAR, and the NAR buffers those packets. Then, referring to Fig. 3, $C_{\mathrm{PAR}}^{\mathrm{duplicate}}$, $C_{\mathrm{tunl}}^{p\cdot\mathrm{fN}}$, and $C_{\mathrm{buff}}^{p\cdot\mathrm{fN}}$ are calculated as follows:

$$C_{\mathrm{PAR}}^{\mathrm{duplicate}} = \mu_h \cdot n_{\mathrm{MNN}} \cdot \mathrm{PD}_{\mathrm{AR-MNN}}^{\mathrm{duplicate}} \cdot (\Delta t_F + t_w(L_{\mathrm{FBack}}))$$
$$C_{\mathrm{tunl}}^{p\cdot\mathrm{fN}} = \mu_h \cdot n_{\mathrm{MNN}} \cdot \mathrm{PD}_{\mathrm{AR-AR}}^{\mathrm{tunnel}} \cdot \left\{T_{\mathrm{HL}}^{p\cdot\mathrm{fN}} - (T_{\mathrm{FAST}} + t_w(L_{\mathrm{FBack}})) - \frac{T_{\mathrm{REG}}}{2}\right\},$$
$$C_{\mathrm{buff}}^{p\cdot\mathrm{fN}} = \mu_h \cdot n_{\mathrm{MNN}} \cdot \lambda_p \cdot (L_{\mathrm{DATA}} + L_{\mathrm{THD}}) \cdot \left\{T_{\mathrm{HL}}^{p\cdot\mathrm{fN}} - (T_{\mathrm{FAST}} + t_w(L_{\mathrm{FBack}})) - \frac{T_{\mathrm{REG}}}{2}\right\}$$

where $\mathrm{PD}_{\mathrm{AR-MNN}}^{\mathrm{duplicate}} = \lambda_p \cdot (\omega \cdot (2L_{\mathrm{DATA}} + L_{\mathrm{THD}}))/(1 - p_{\mathrm{wlf}})$ and $\mathrm{PD}_{\mathrm{AR-AR}}^{\mathrm{tunnel}} = \lambda_p \cdot d_{\mathrm{AR-AR}} \cdot (L_{\mathrm{DATA}} + 2L_{\mathrm{THD}})$.

In the reactive mode of fNEMO, $C_{\mathrm{PD}}^{r\cdot\mathrm{fN}}$ consists of the tunneling cost $C_{\mathrm{tunl}}^{r\cdot\mathrm{fN}}$ and the packet-loss cost $C_{\mathrm{loss}}^{r\cdot\mathrm{fN}}$, and is calculated as follows:

$$C_{\mathrm{PD}}^{r\cdot\mathrm{fN}} = \tau \cdot C_{\mathrm{tunl}}^{r\cdot\mathrm{fN}} + \beta \cdot C_{\mathrm{loss}}^{r\cdot\mathrm{fN}}.$$

In the reactive mode of fNEMO, all packets destined for MNNs are lost until the PAR receives the FBU message; then, they are tunneled to the NAR. Thus, referring to Fig. 3, $C_{\mathrm{tunl}}^{r\cdot\mathrm{fN}}$ and $C_{\mathrm{loss}}^{r\cdot\mathrm{fN}}$ are expressed as follows:

$$C_{\mathrm{tunl}}^{r\cdot\mathrm{fN}} = \mu_h \cdot n_{\mathrm{MNN}} \cdot \mathrm{PD}_{\mathrm{AR-AR}}^{\mathrm{tunnel}} \cdot \left(t_d(L_{\mathrm{FBack}}) + t_w(L_{\mathrm{DATA}}) + \frac{T_{\mathrm{REG}}}{2}\right),$$
$$C_{\mathrm{loss}}^{r\cdot\mathrm{fN}} = \mu_h \cdot n_{\mathrm{MNN}} \cdot \mathrm{PD}_{\mathrm{CN-AR}}^{\mathrm{previous}} \cdot \left\{T_{\mathrm{L2}} + (T_{\mathrm{NEW}}^{\mathrm{re}} - t_d(L_{\mathrm{FBack}}) - t_w(L_{\mathrm{DATA}}))\right\}.$$

Similar to fNEMO, EfNEMO is divided into the predictive mode and the reactive mode. Then, the signaling overhead, $C_{\mathrm{SOH}}^{\mathrm{EfN}}$ and the packet delivery cost $C_{\mathrm{PD}}^{\mathrm{EfN}}$ are expressed as follows:

$$C_{\mathrm{SOH}}^{\mathrm{EfN}} = (1 - p_{\mathrm{pmf}}) \cdot C_{\mathrm{SOH}}^{p\cdot\mathrm{EfN}} + p_{\mathrm{pmf}} \cdot C_{\mathrm{SOH}}^{r\cdot\mathrm{EfN}}$$
$$C_{\mathrm{PD}}^{\mathrm{EfN}} = (1 - p_{\mathrm{pmf}}) \cdot C_{\mathrm{PD}}^{p\cdot\mathrm{EfN}} + p_{\mathrm{pmf}} \cdot C_{\mathrm{PD}}^{r\cdot\mathrm{EfN}}$$

where $C_{\mathrm{SOH}}^{p\cdot\mathrm{EfN}}$, $C_{\mathrm{SOH}}^{r\cdot\mathrm{EfN}}$, $C_{\mathrm{PD}}^{p\cdot\mathrm{EfN}}$, and $C_{\mathrm{PD}}^{r\cdot\mathrm{EfN}}$ are the signaling overheads and the packet delivery costs for the predictive mode and the reactive mode of EfNEMO, respectively. Referring to Fig. 3, $C_{\mathrm{SOH}}^{p\cdot\mathrm{EfN}}$ and $C_{\mathrm{SOH}}^{r\cdot\mathrm{EfN}}$ are obtained as follows:

$$C_{\mathrm{SOH}}^{p\cdot\mathrm{EfN}} = \mu_h \cdot \left(S_{\mathrm{FAST}}^{\mathrm{EfN}} + \frac{S_{\mathrm{MD}}}{2} + S_{\mathrm{REG}}\right)$$
$$C_{\mathrm{SOH}}^{r\cdot\mathrm{EfN}} = \mu_h \cdot \left(S_{\mathrm{NEW}}^{r\cdot\mathrm{EfN}} + S_{\mathrm{REG}}\right)$$

where $S_{\mathrm{FAST}}^{\mathrm{EfN}} = S_{\mathrm{FAST}}^{\mathrm{fN}} + (\omega \cdot L_{\mathrm{TBU}})/(1 - p_{\mathrm{wlf}}) + d_{\mathrm{AR-AR}} \cdot L_{\mathrm{TBU}} + d_{\mathrm{HA-AR}} \cdot L_{\mathrm{TBU}}$ and $S_{\mathrm{FAST}}^{r\cdot\mathrm{EfN}} = S_{\mathrm{FAST}}^{r\cdot\mathrm{fN}} + (\omega \cdot L_{\mathrm{TBU}})/$

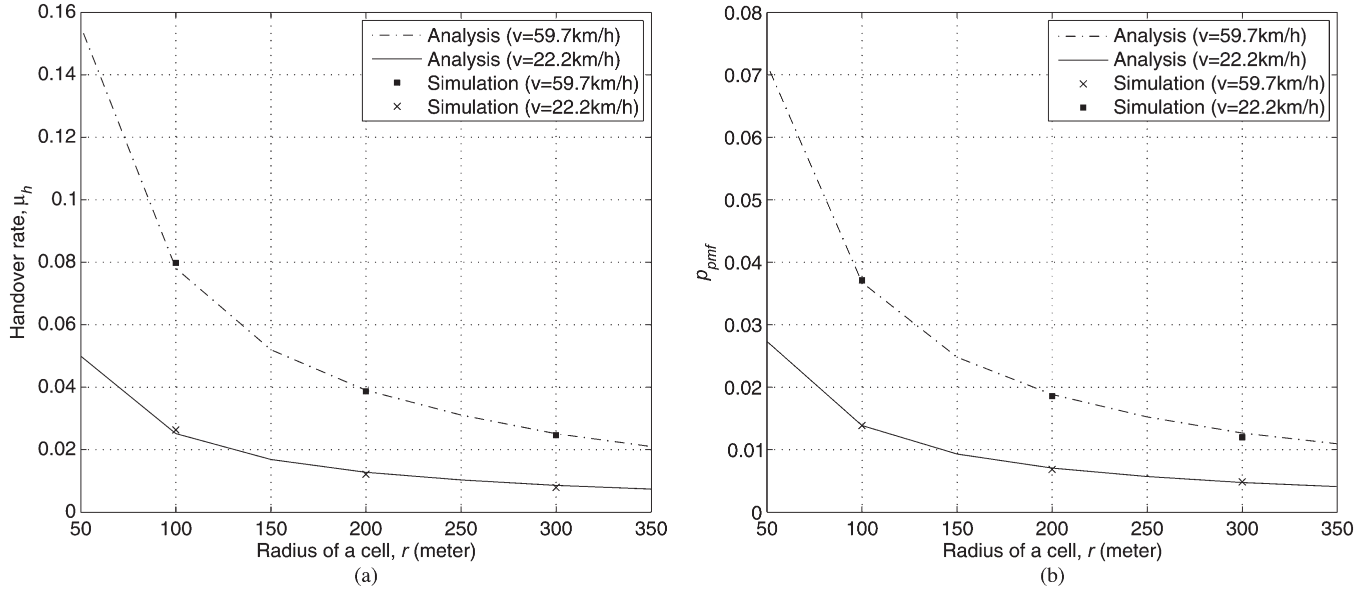

Fig. 7. Results of the mobility model concerning the average handover rate μ_h and the probability of predictive mode failure p_{pmf}. (a) Average handover rate. (b) Probability of predictive mode failure.

$(1 - p_{\mathrm{wlf}}) + d_{\mathrm{AR-AR}} \cdot L_{\mathrm{TBU}} + d_{\mathrm{HA-AR}} \cdot L_{\mathrm{TBU}}$ because the signaling costs of EfNEMO are added to those of fNEMO by the cost of transmitting the TBU message.

In EfNEMO, generally, the tunneling cost is not considered because packets are delivered to the NAR directly. However, when the MR is too far from the HA, the TBU message may not arrive at the HA during T_{FAST}. In this case, the tunnel between the PAR and the NAR is used as in fNEMO. Then, $C_{\mathrm{PD}}^{p\cdot\mathrm{EfN}}$ and $C_{\mathrm{PD}}^{r\cdot\mathrm{EfN}}$ are expressed as follows:

$$C_{\mathrm{PD}}^{p\cdot\mathrm{EfN}} = C_{\mathrm{PAR}}^{\mathrm{duplicate}} + \beta \cdot C_{\mathrm{buff}}^{p\cdot\mathrm{EfN}} + \tau \cdot C_{\mathrm{tunl}}^{p\cdot\mathrm{EfN}}$$
$$C_{\mathrm{PD}}^{r\cdot\mathrm{EfN}} = \epsilon \cdot C_{\mathrm{loss}}^{r\cdot\mathrm{EfN}}$$

since the HA starts to forward packets to the NAR when it receives the TBU message. In the predictive mode of EfNEMO, the PAR transfers duplicate packets to the NAR and the MR when it receives the HAck message. The NAR buffers packets from the HA during the handover. In addition, if the TBU message is not delivered to the HA during T_{FAST}, packets destined for the MR are tunneled as in fNEMO. Thus, in the predictive mode of EfNEMO, the buffering cost $C_{\mathrm{buff}}^{p\cdot\mathrm{EfN}}$ and the tunneling cost $C_{\mathrm{tunl}}^{p\cdot\mathrm{EfN}}$ are expressed as follows:

$$C_{\mathrm{buff}}^{p\cdot\mathrm{EfN}} = \mu_h \cdot n_{\mathrm{MNN}} \cdot \lambda_p \cdot (L_{\mathrm{DATA}} + L_{\mathrm{THD}}) \cdot \left\{ T_{\mathrm{HL}}^{\mathrm{EfN}} - (T_{\mathrm{FAST}} + t_w(L_{\mathrm{FBack}})) - \frac{T_{\mathrm{NEW}}}{2} \right\}$$
$$C_{\mathrm{tunl}}^{p\cdot\mathrm{EfN}} = \mu_h \cdot n_{\mathrm{MNN}} \cdot \mathrm{PD}_{\mathrm{AR-AR}}^{\mathrm{tunnel}} \cdot \min \left(\max\left(t_d(L_{\mathrm{TBU}}) \cdot d_{\mathrm{HA-AR}} - t_w(L_{\mathrm{FBack}}),\, 0\right) T_{\mathrm{L2}} + T_{\mathrm{NEW}} + \frac{T_{\mathrm{REG}}}{2} \right).$$

In the reactive mode of EfNEMO, packets are lost until the HA receives the TBU message. Then, $C_{\mathrm{loss}}^{r\cdot\mathrm{EfN}}$ is obtained as follows:

$$C_{\mathrm{loss}}^{r\cdot\mathrm{EfN}} = \mu_h \cdot n_{\mathrm{MNN}} \cdot \mathrm{PD}_{\mathrm{CN-AR}}^{\mathrm{previous}} \cdot \{T_{\mathrm{L2}} + t_w(L_{\mathrm{UNA}} + L_{\mathrm{FBU}} + L_{\mathrm{TBU}}) + d_{\mathrm{HA-AR}} \cdot t_d(L_{\mathrm{TBU}})\}.$$

V. Numerical Results

Here, we compare the numerical performance of NEMO, fNEMO, and EfNEMO in terms of the overall cost and the handover latency. Additionally, we simulated fNEMO and EfNEMO in an urban scenario to focus on the comparison of EfNEMO with fNEMO. To show a simulation scenario in which nodes move according to vehicular patterns in urban area, we use ns-2 and Matlab. For urban area simulation, we use the ManhattanGrid model by using Bonnmotion [37], which is a mobility scenario generation and analysis tool. In simulation, APs are distributed as in Fig. 5 to simulate in similar environment to the analytical model. Through simulation, we show that the results of simulation are similar to those of analysis, as shown in figures of analysis results.

A. Mobility Model

To obtain the average handover rate μ_h and the probability of predictive mode failure p_{pmf}, analytical models are evaluated, and simulation is performed using various network parameters, such as the radius of a cell r and the velocity of the vehicle v. Fig. 7(a) and (b) shows μ_h and p_{pmf} as functions of r and v. μ_h and p_{pmf} increase as r decreases or as v increases, whereas they decrease as r increases or v decreases. For urban and urban expressway scenarios, we use 22.2 and 59.7 km/h, which are average velocities in urban streets and urban expressways in Seoul, Korea, respectively [38], [39]. In particular, to analyze and simulate an urban expressway scenario, the parameters for the mobility model are modified. For example, we assume that

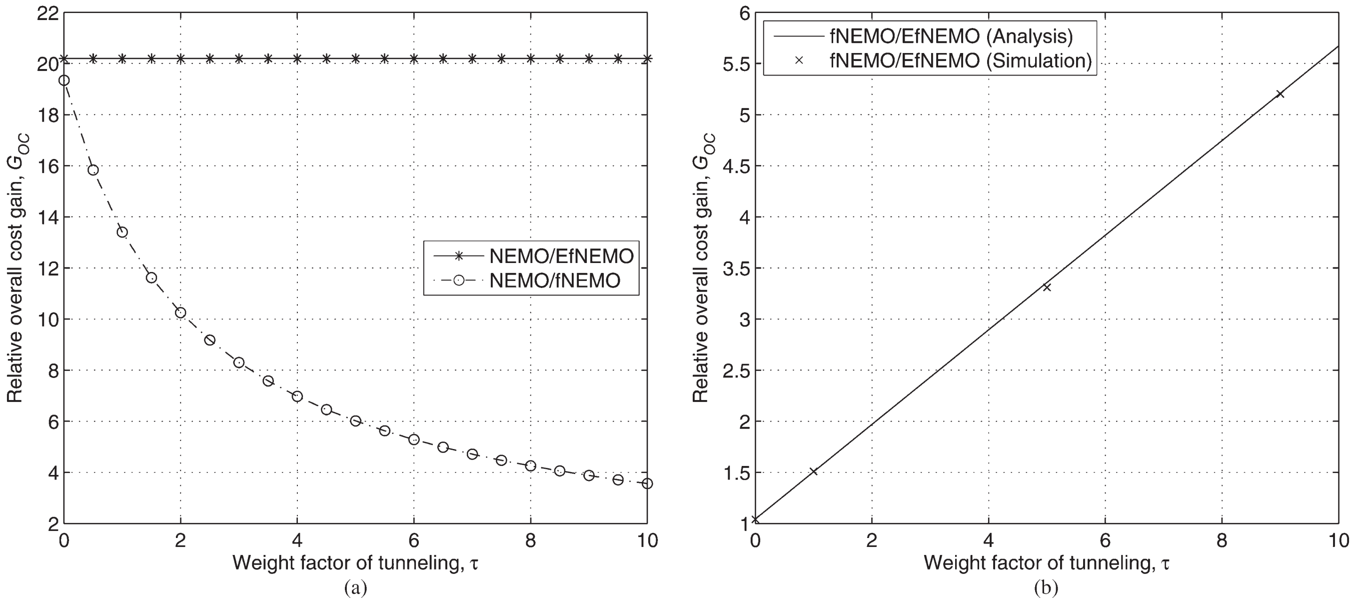

Fig. 8. Relative overall cost gains as a function of the weight factor for tunneling τ. (a) $G_{\mathrm{OC}}^{\mathrm{NEMO/fNEMO}}$ and $G_{\mathrm{OC}}^{\mathrm{NEMO/EfNEMO}}$. (b)$G_{\mathrm{OC}}^{\mathrm{fNEMO/EfNEMO}}$.

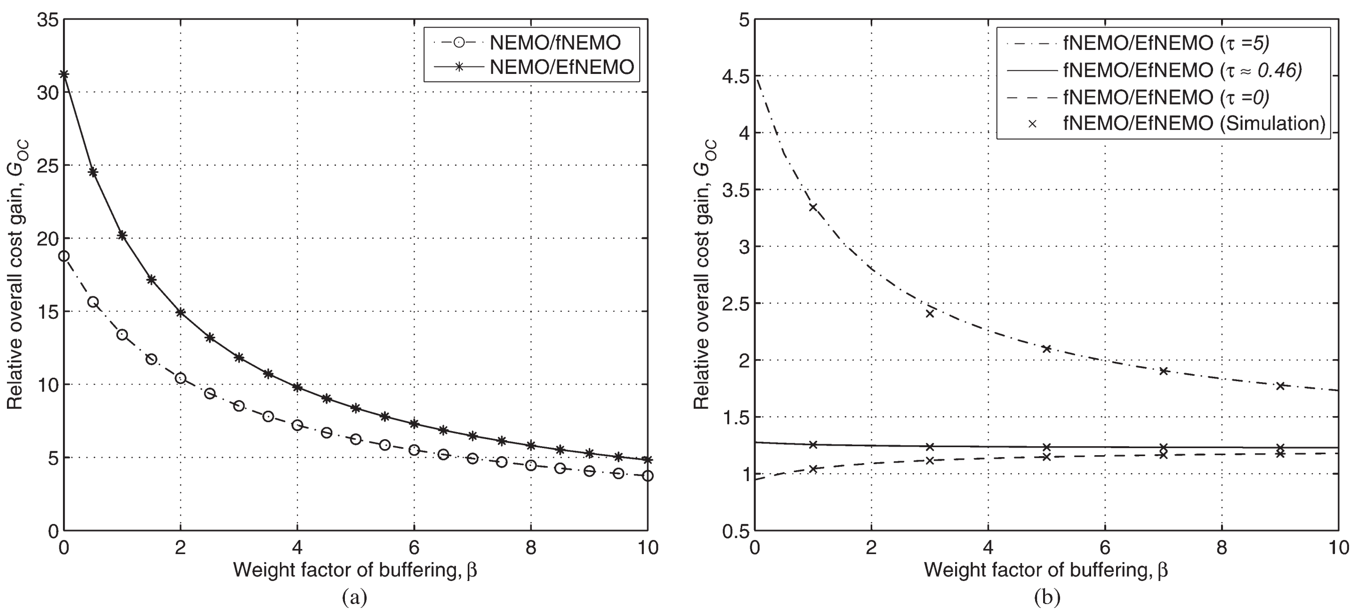

Fig. 9. Relative overall cost gains as a function of the weight factor for buffering β. (a) $G_{\mathrm{OC}}^{\mathrm{NEMO/fNEMO}}$ and $G_{\mathrm{OC}}^{\mathrm{NEMO/EfNEMO}}$. (b) $G_{\mathrm{OC}}^{\mathrm{fNEMO/EfNEMO}}$.

$D_v = 0.1$ km, $S_v = 0.1$ km for analysis, and the number of vertical roads to be 1 for simulation.

B. Relative Overall Cost Gain

For the purpose of comparison, we define the relative overall cost gains as follows:

$$G_{\mathrm{OC}}^{\mathrm{NEMO/fNEMO}} = \frac{C_{\mathrm{SOH}}^{\mathrm{NEMO}} + C_{\mathrm{PD}}^{\mathrm{NEMO}}}{C_{\mathrm{SOH}}^{\mathrm{fN}} + C_{\mathrm{PD}}^{\mathrm{fN}}}$$
$$G_{\mathrm{OC}}^{\mathrm{NEMO/EfNEMO}} = \frac{C_{\mathrm{SOH}}^{\mathrm{NEMO}} + C_{\mathrm{PD}}^{\mathrm{NEMO}}}{C_{\mathrm{SOH}}^{\mathrm{EfN}} + C_{\mathrm{PD}}^{\mathrm{EfN}}}$$
$$G_{\mathrm{OC}}^{\mathrm{fNEMO/EfNEMO}} = \frac{C_{\mathrm{SOH}}^{\mathrm{fN}} + C_{\mathrm{PD}}^{\mathrm{fN}}}{C_{\mathrm{SOH}}^{\mathrm{EfN}} + C_{\mathrm{PD}}^{\mathrm{EfN}}}$$

where $G_{\mathrm{OC}}^{\mathrm{NEMO/fNEMO}}$ and $G_{\mathrm{OC}}^{\mathrm{NEMO/EfNEMO}}$ are the relative overall cost gains of fNEMO and EfNEMO to NEMO, respectively, and $G_{\mathrm{OC}}^{\mathrm{fNEMO/EfNEMO}}$ is the relative overall cost gain of EfNEMO to fNEMO. Parameters used in this analysis are defined as follows: $D_h = 36$ km, $D_v = 24$ km, $U_{\max} = 4$ s, $S_h = 0.1$ km, $S_v = 0.1$ km, $r = 300$ m [40], $v = 22.2$ km/h, $K = 3$, $d_{\mathrm{CN-HA}} = 5$, $d_{\mathrm{HA-AR}} = 5$, $d_{\mathrm{AR-AR}} = 1$, $p_{\mathrm{wlf}} = 0.5$, $\omega_q = 0.5$, $T_{\mathrm{wl}} = 2$ ms, $T_{\mathrm{wd}} = 0.5$ ms, $T_p = 0.5$ ms, $B_{\mathrm{wl}} = 54$ Mb/s, $B_{\mathrm{wd}} = 1$ Gb/s, $\Delta t_F = 0$, $T_{\mathrm{L2}} = 243.9$ ms [41], $T_{\mathrm{DAD}} = 1000$ ms [27], $n_{\mathrm{MNN}} = 5$, $\lambda_p = 50$ packets$/s$, $\eta = 1$, $\omega = 10$, $\tau = 1$, $\beta = 1$, $\epsilon = 1$, $L_{\mathrm{NS}} = L_{\mathrm{RS}} = L_{\mathrm{BA}} = L_{\mathrm{RSP}} = L_{\mathrm{FBack}} = L_{\mathrm{HI}} = L_{\mathrm{HAck}} = L_{\mathrm{UNA}} = 52$ B, $L_{\mathrm{RA}} = 92$, $L_{\mathrm{BU}} = L_{\mathrm{FBU}} = L_{\mathrm{TBU}} = 72$ B, and $L_{\mathrm{THD}} = 40$ B [34], [35], [42].

Fig. 8 shows the relative overall cost gains as a function of the weight factor for tunneling τ. τ indicates the degree of traffic

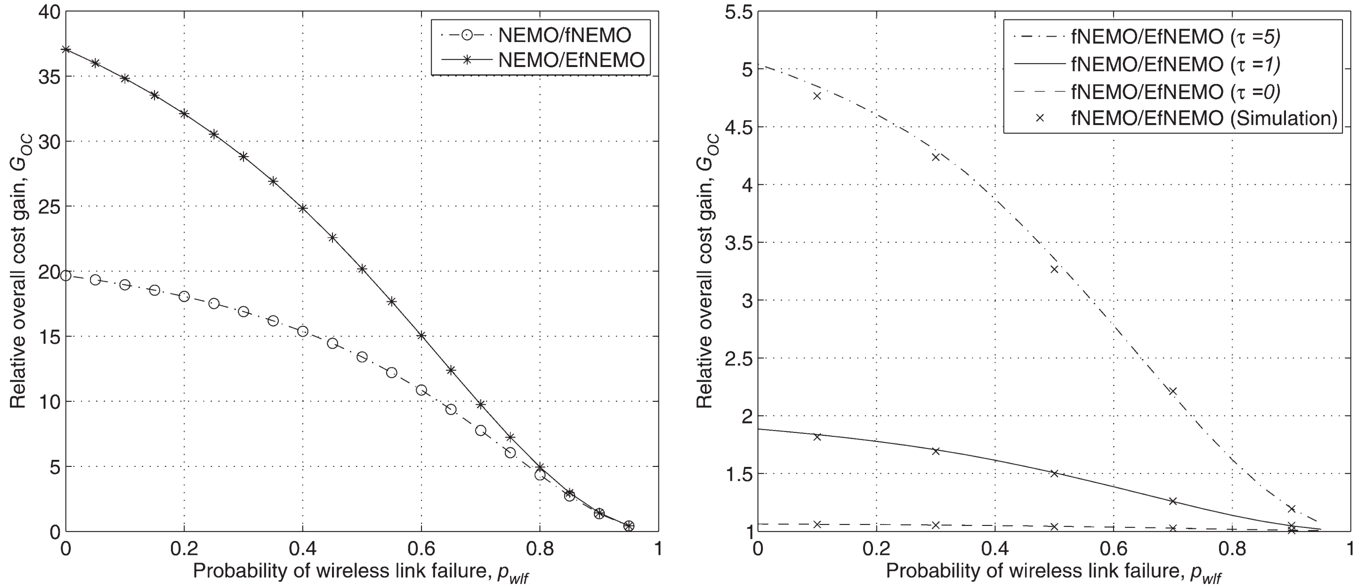

(a) (b)

Fig. 10. Relative overall cost gains as a function of the probability of wireless link failure p_{wlf}. (a)$G_{\mathrm{OC}}^{\mathrm{NEMO/fNEMO}}$ and $G_{\mathrm{OC}}^{\mathrm{NEMO/EfNEMO}}$. (b) $G_{\mathrm{OC}}^{\mathrm{fNEMO/EfNEMO}}$.

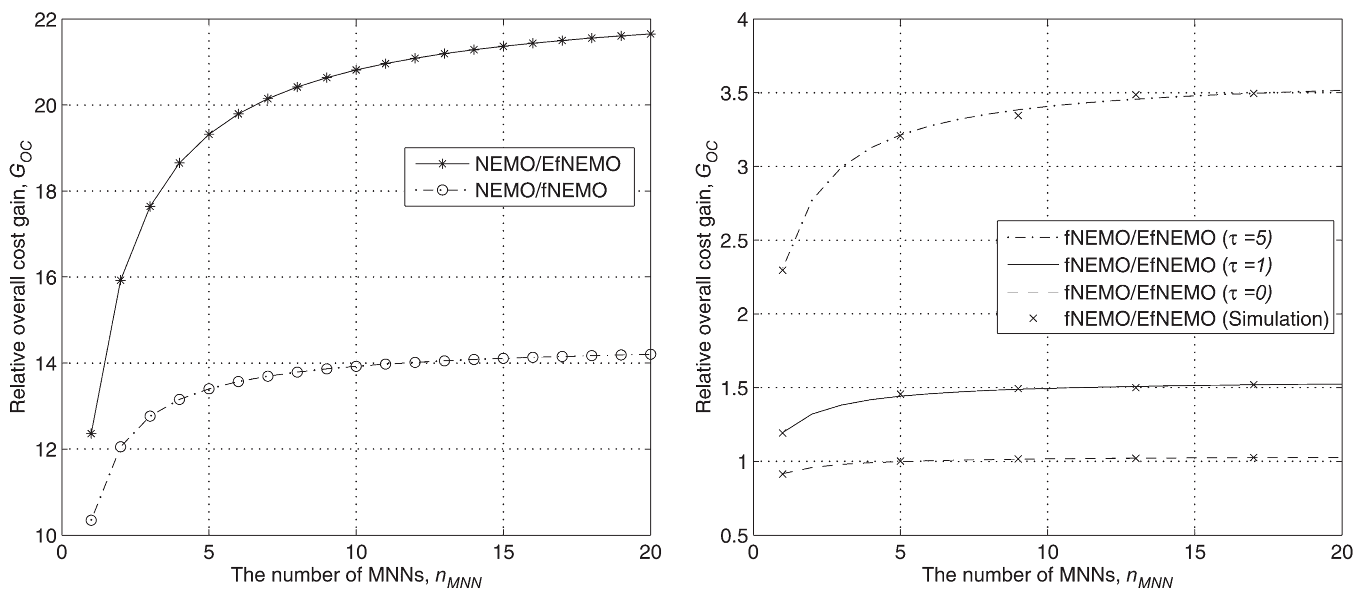

(a) (b)

Fig. 11. Relative overall cost gains as a function of the number of MNNs n_{MNN}. (a) $G_{\mathrm{OC}}^{\mathrm{NEMO/fNEMO}}$ and $G_{\mathrm{OC}}^{\mathrm{NEMO/EfNEMO}}$. (b) $G_{\mathrm{OC}}^{\mathrm{fNEMO/EfNEMO}}$.

density over the link between the PAR and the NAR. Additionally, road traffic characteristics can be indirectly expressed by τ. When road traffic is high, the number of vehicles moving between the same ARs can increase, so that the link between those ARs can be overloaded. This is because we assumed that the number of MNs in an MR and a packet arrival rate for each MNs are fixed, and an MR moves between ARs. Therefore, τ can imply road traffic characteristics. In Fig. 8(a), fNEMO and EfNEMO outperform NEMO. However, the overall cost gain of fNEMO decreases as τ increases, whereas that of EfNEMO remains almost the same, regardless of τ. This is due to the tunneling cost of fNEMO that incurs high packet delivery cost. Thus, as shown in Fig. 8(b), EfNEMO significantly enhances the handover performance of fNEMO because it eliminates the tunneling cost of fNEMO.

We further consider the buffering cost to calculate the overall costs of fNEMO and EfNEMO, which was not usually included in the performance evaluation in previous studies. Fig. 9(a) shows the relative overall cost gains of fNEMO and EfNEMO to NEMO as a function of the weight factor for buffering β. When β is low, both fNEMO and EfNEMO improve the handover performance of NEMO. The overall cost gains of fNEMO and EfNEMO to NEMO decrease as β increases because NEMO does not use any buffering. As shown in Fig. 9(b), the handover performance of EfNEMO improves as β decreases when $\tau > 0.46$, whereas it increases as β increases when $\tau <$

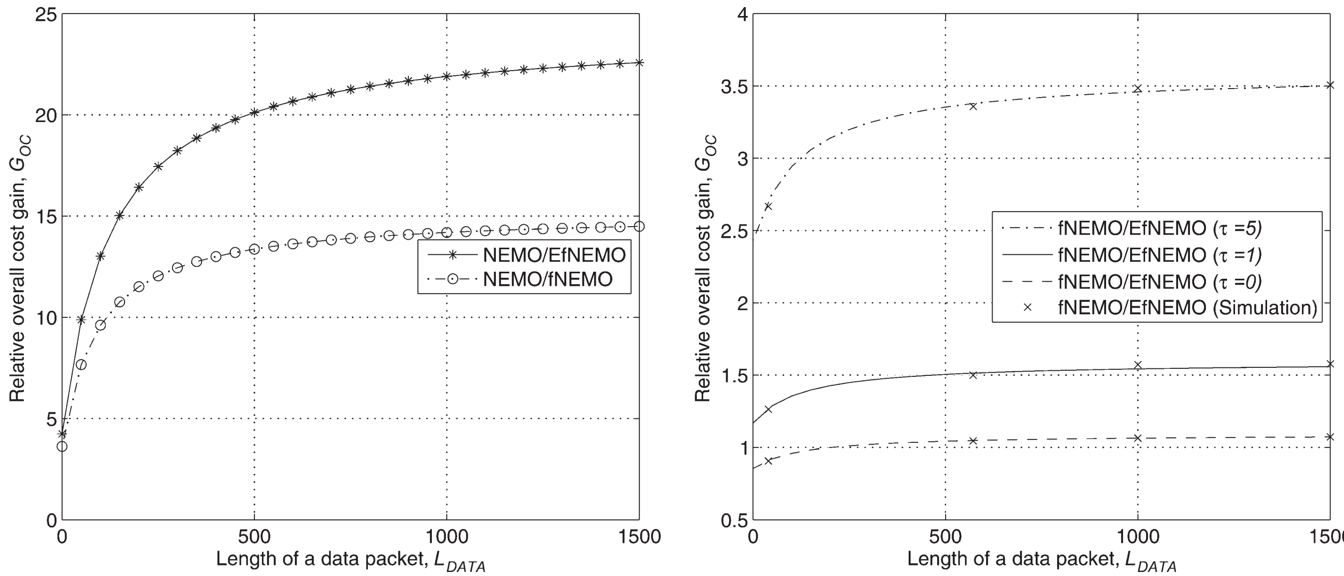

(a) (b)

Fig. 12. Relative overall cost gains as a function of the length of a data packet L_{DATA}. (a) $G_{\mathrm{OC}}^{\mathrm{NEMO/fNEMO}}$ and $G_{\mathrm{OC}}^{\mathrm{NEMO/EfNEMO}}$. (b) $G_{\mathrm{OC}}^{\mathrm{fNEMO/EfNEMO}}$.

0.46. The main reason for this phenomenon is that the tunneling cost is high compared with the buffering cost when τ is high.

In fNEMO and EfNEMO, additional signaling messages, such as the FBU and FBack messages, are necessary. The transmission cost of these messages is mainly influenced by p_{wlf}. As shown in Fig. 10(a), if p_{wlf} is small, i.e., the wireless channel error is insignificant, fNEMO and EfNEMO dramatically enhance the handover performance of NEMO. However, the relative overall cost gains of fNEMO and EfNEMO decrease as p_{wlf} increases. Fig. 10(b) shows the relative overall cost gain of EfNEMO to fNEMO with respect to p_{wlf}. EfNEMO greatly enhances the handover performance of fNEMO when p_{wlf} is low. The overall cost gain of EfNEMO decreases as p_{wlf} increases because EfNEMO is more affected by p_{wlf} due to the TBU message. Additionally, EfNEMO greatly enhances the handover performance of fNEMO when τ is high.

Fig. 11(a) shows the relative overall cost gains of fNEMO and EfNEMO as a function of n_{MNN}. As n_{MNN} increases, a handover performance of fNEMO and EfNEMO becomes better because the cost of packet loss in NEMO notably increases. As shown in Fig. 11(b), EfNEMO enhances the handover performance of fNEMO even when n_{MNN} is large.

The data packet length varies. For example, a 40-B packet is for Transmission Control Protocol (TCP) acknowledgments, and 572- and 1500-B packets are the most common default message transmission units [43]. In Fig. 12(a), the relative overall cost gains of fNEMO and EfNEMO to NEMO with respect to L_{DATA} are plotted. Since the packet delivery cost depends on L_{DATA}, the handover performances of fNEMO and EfNEMO to NEMO increase as L_{DATA} increases. Fig. 12(b) shows that the handover performance of EfNEMO increases as L_{DATA} increases. The reason is the same as that for Fig. 11(b).

Fig. 13 shows the relative overall cost gains of EfNEMO as a function of the distance ratio between the HA and the MR and between the PAR and the NAR. This ratio is $d_{\mathrm{HA-MR}}/d_{\mathrm{AR-AR}}$.

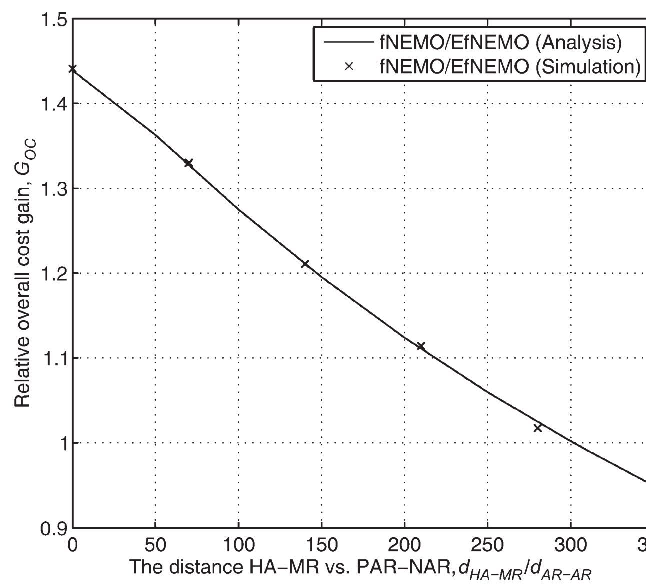

Fig. 13. Relative overall cost gains as a function of the distance ratio between HA–MR and PAR–NAR $d_{\mathrm{HA-MR}}/d_{\mathrm{AR-AR}}$.

In general, the handover performance of EfNEMO is higher than that of fNEMO when this ratio is small. However, the handover performance of EfNEMO decreases as this ratio increases since the tunnel between PAR and NAR is used until the TBU message is processed in the HA. If this ratio is larger than 300, the handover performance of EfNEMO becomes lower than that of fNEMO. That is, when the MR is too far from the HA, fNEMO may provide a better performance. In this case, localized HA schemes, such as hierarchical MIPv6 [44] and proxy MIPv6 [45], should be adopted in EfNEMO. Schemes to combine fNEMO and EfNEMO with proxy MIPv6 have been studied by some researchers [46], [47]. However, since the MR is not too far from the HA in usual environments, EfNEMO normally outperforms fNEMO.

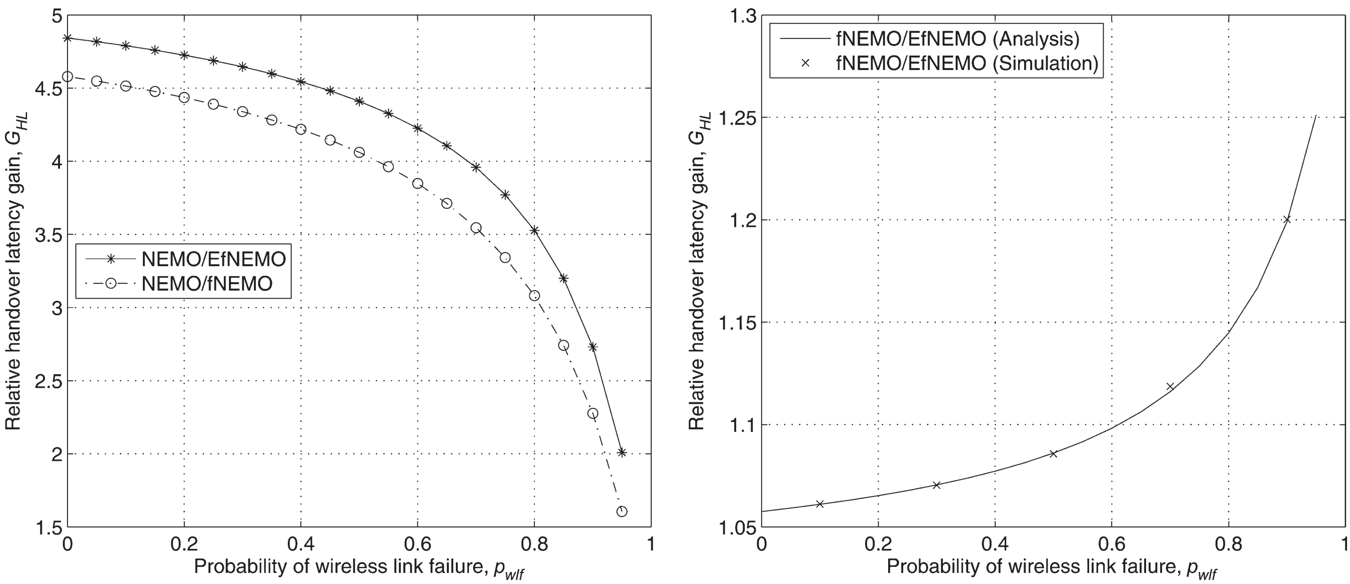

(a) (b)

Fig. 14. Relative handover latency gains as a function of p_{wlf}. (a) $G_{\mathrm{HL}}^{\mathrm{NEMO/fNEMO}}$ and $G_{\mathrm{HL}}^{\mathrm{NEMO/EfNEMO}}$. (b) $G_{\mathrm{HL}}^{\mathrm{fNEMO/EfNEMO}}$.

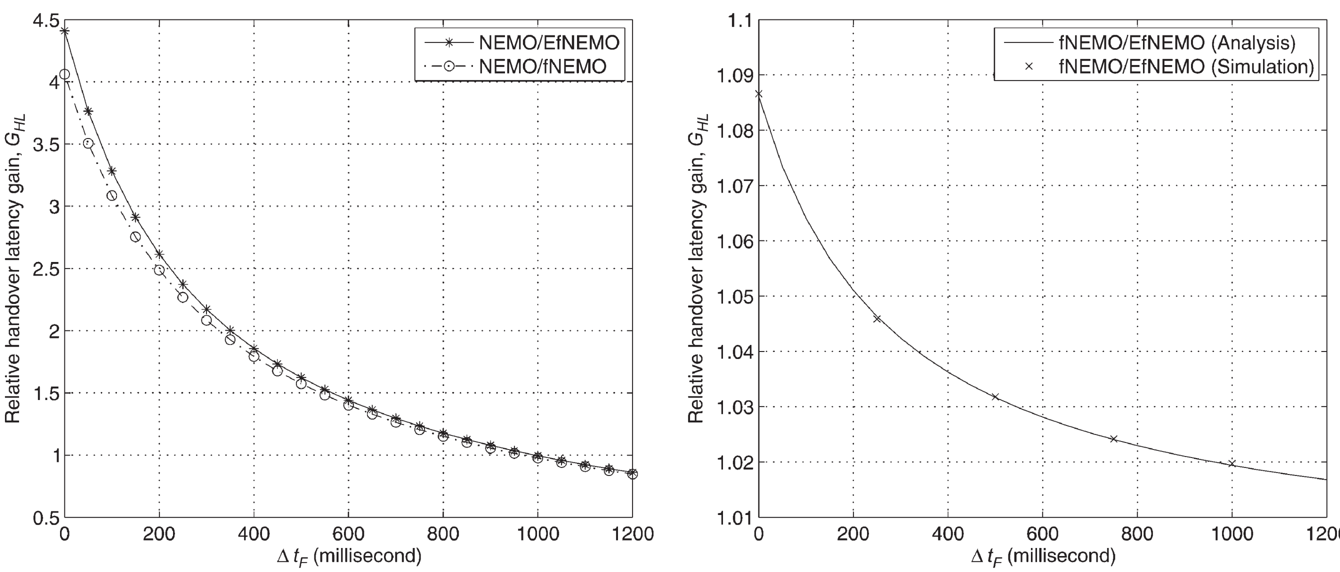

(a) (b)

Fig. 15. Relative handover latency gains as a function of Δt_F. (a) $G_{\mathrm{HL}}^{\mathrm{NEMO/fNEMO}}$ and $G_{\mathrm{HL}}^{\mathrm{NEMO/EfNEMO}}$. (b) $G_{\mathrm{HL}}^{\mathrm{fNEMO/EfNEMO}}$.

C. Relative Handover Latency Gain

To compare the performance of NEMO, fNEMO, and EfNEMO in terms of the handover latency, we define the relative handover latency gains as follows:

$$G_{\mathrm{HL}}^{\mathrm{NEMO/fNEMO}} = \frac{T_{\mathrm{HL}}^{\mathrm{NEMO}}}{T_{\mathrm{HL}}^{\mathrm{fN}}},$$
$$G_{\mathrm{HL}}^{\mathrm{NEMO/EfNEMO}} = \frac{T_{\mathrm{HL}}^{\mathrm{NEMO}}}{T_{\mathrm{HL}}^{\mathrm{EfN}}},$$
$$G_{\mathrm{HL}}^{\mathrm{fNEMO/EfNEMO}} = \frac{T_{\mathrm{HL}}^{\mathrm{fN}}}{T_{\mathrm{HL}}^{\mathrm{EfN}}}$$

where $G_{\mathrm{HL}}^{\mathrm{NEMO/fNEMO}}$ and $G_{\mathrm{HL}}^{\mathrm{NEMO/EfNEMO}}$ are the relative handover latency gains of fNEMO and EfNEMO to NEMO, respectively, and $G_{\mathrm{HL}}^{\mathrm{fNEMO/EfNEMO}}$ is the relative handover latency gain of EfNEMO to fNEMO.

Fig. 14(a) plots the relative handover latency gains of fNEMO and EfNEMO to NEMO with respect to p_{wlf}. When p_{wlf} is small, fNEMO and EfNEMO outperform NEMO. The relative handover latency gains of fNEMO and EfNEMO decrease as p_{wlf} increases because a large value of p_{wlf} increases a wireless link delay. As shown in Fig. 14(b), EfNEMO improves the handover performance of fNEMO even when p_{wlf} is large because EfNEMO uses the wireless link less frequently.

In our numerical results, we assume $\Delta t_F = 0$ because there is good synchronization between the layer-2 and layer-3 handovers [34]. However, in practice, there is no way to know the exact time instant when the layer-2 handover begins after the MR receives the FBack message. Thus, we show the impact of

Δt_F in terms of the handover latency in Fig. 15. The relative handover latency gains of fNEMO and EfNEMO to NEMO increase as Δt_F decreases because a small Δt_F shortens the handover latency in fNEMO and EfNEMO. When $\Delta t_F >$ 1000 ms, the handover latencies of fNEMO and EfNEMO are longer than that of NEMO because $T_{\text{DAD}} = 1000$ ms, which is a critical delay in NEMO. As shown in Fig. 15(b), EfNEMO improves the handover performance of fNEMO even when Δt_F is large because there is no T_{REG} in EfNEMO.

VI. Conclusion

To reduce packet loss and handover latency in NEMO, a fast network mobility management protocol for ITS standards, i.e., fNEMO, was proposed in earlier works. We have pointed out that fNEMO has a significant tunneling burden, which can cause significant packet loss and handover latency. To eliminate the tunneling burden of fNEMO, we have proposed EfNEMO, which is an efficient fast handover mechanism for NEMO. We investigated the overall cost and the handover latency of EfNEMO. Both our analytical and simulation results show that the handover performance of EfNEMO significantly outperforms those of fNEMO and NEMO. We expect that EfNEMO can be used as an efficient network mobility protocol for ITS.

References

[1] S. Cespedes, X. Shen, and C. Lazo, "IP mobility management for vehicular communication networks: Challenges and solutions," *IEEE Commun. Mag.*, vol. 49, no. 5, pp. 187–194, May 2011.

[2] K. Zhu, D. Niyato, P. Wang, E. Hossain, and D. I. Kim, "Mobility and handoff management in vehicular networks: A survey," *Wireless Commun. Mob. Comput.*, vol. 11, no. 4, pp. 459–476, Apr. 2011.

[3] I. Soto, C. J. Bernardos, M. Calderon, A. Banchs, and A. Azcorra, "NEMO-enabled localized mobility support for Internet access in automotive scenarios," *IEEE Commun. Mag.*, vol. 47, no. 5, pp. 152–159, May 2009.

[4] V. Devarapalli, R. Wakikawa, A. Petrescu, and P. Thubert, Network mobility (NEMO) basic support protocol, RFC 3963, Jan. 2005.

[5] T. Ernst, "The information technology era of the vehicular industry," *ACM SIGCOMM Comput. Commun. Rev.*, vol. 36, no. 2, pp. 49–52, Apr. 2006.

[6] C. Perkins, D. Johnson, and J. Arkko, Mobility support in IPv6, RFC 6275, Jul. 2011.

[7] ISO Draft DIS 21210, Intelligent transport systems—Communications access for land mobiles (CALM)—IPv6 networking, Feb. 2009.

[8] GeoNet Project, Dec. 2011. [Online]. Available: http://www.geonet-project.eu

[9] ETSI TS 102 636-3, v1.1.1, Intelligent Transport Systems (ITS), Vehicular communications, GeoNetworking, Part 3: Network architecture, Mar. 2010.

[10] ETSI TS 102 636-4-1,v0.0.9, Intelligent Transport Systems (ITS), Vehicular communications, Part 4: Geographical addressing and forwarding for point-to-point and point-to-multipoint communications, Sub-Part 1: Media-independent functionality, Nov. 2010.

[11] Q. B. Mussabbir, W. Yao, Z. Niu, and X. Fu, "Optimized FMIPv6 using IEEE 802.21 MIH services in vehicular networks," *IEEE Trans. Veh. Technol.*, vol. 56, no. 1, pp. 3397–3407, Nov. 2007.

[12] L. Zhong, F. Liu, X. Wang, and Y. Ji, "Fast handover scheme for supporting network mobility in IEEE 802.16e BWA system," in *Proc. Int. Conf. WiCom*, Shanghai, China, 2007, pp. 1757–1760.

[13] S. J. Yoo, S. J. Choi, and D. Su, "Analysis of fast handover mechanisms for hierarchical mobile IPv6 network mobility," *Wireless Pers. Commun.*, vol. 48, no. 2, pp. 215–238, Jan. 2009.

[14] L. Qingbo, Z. Xuejun, and Z. Liang, "A mobility management mechanism in aeronautical telecommunication network," in *Proc. IET Int. CCWMC*, 2009, pp. 594–597.

[15] B. A. Mohammed and T. C. Wan, "Modified fast-integrated light-NEMOv6 handoff in IEEE 802.16e BWA networks," in *Proc. 2nd Int. Conf. NETAPPS*, 2010, pp. 182–187.

[16] R. Chaki and N. G. Niyogi, "An improved scheme towards fast handover in a hierarchical mobile network," in *Proc. URSI General Assembly Sci. Symp.*, 2011, pp. 1–4.

[17] RFC 5568, Mobile IPv6 Fast Handovers, Jul. 2009.

[18] M. Calderon, C. J. Bernardos, M. Bagnulo, I. Soto, and A. de la Oliva, "Design and experimental evaluation of a route optimization solution for NEMO," *IEEE J. Sel. Areas Commun.*, vol. 24, no. 9, pp. 1702–1716, Sep. 2006.

[19] H. Petander, E. Perera, K.-C. Lan, and A. Seneviratne, "Measuring and improving the performance of network mobility management in IPv6 networks," *IEEE J. Sel. Areas Commun.*, vol. 24, no. 9, pp. 1671–1681, Sep. 2006.

[20] I. C. Chang and C. H. Chou, "HCoP-B: A hierarchical care-of prefix with BUT scheme for nested mobile networks," *IEEE Trans. Veh. Technol.*, vol. 58, no. 6, pp. 2942–2965, Jul. 2009.

[21] S. Pack, T. Kwon, Y. Choi, and E. Paik, "An adaptive network mobility support protocol in hierarchical mobile IPv6 networks," *IEEE Trans. Veh. Technol.*, vol. 58, no. 7, pp. 3627–3639, Sep. 2009.

[22] C. M. Huang, C. H. Lee, and J. R. Zheng, "A novel SIP-based route optimization for network mobility," *IEEE J. Sel. Areas Commun.*, vol. 24, no. 9, pp. 1682–1691, Sep. 2009.

[23] H. J. Lim, M. Kim, J. H. Lee, and T. M. Chung, "Route optimization in nested NEMO: Classification, evaluation, and analysis from NEMO fringe stub perspective," *IEEE Trans. Mobile Comput.*, vol. 8, no. 11, pp. 1554–1572, Nov. 2009.

[24] A. Z. M. Shahriar, M. Atiquzzaman, and W. Ivancic, "Route optimization in network mobility: Solutions, classification, comparison, and future research directions," *IEEE Commun. Surveys Tut.*, vol. 12, no. 1, pp. 24–38, 1st Quarter, 2010.

[25] S. Ryu and Y. Mun, "The tentative and early binding update for mobile IPv6 fast handover," in *Proc. MSN*, vol. 3794, *Lecture Notes Comput. Sci.*, Dec. 2005, pp. 825–835.

[26] S. Ryu and Y. Mun, "A scheme to enhance TEBU scheme of fast handovers for mobile IPv6," in *Proc. Int. Conf. Embedded Software and Systems*, vol. 4523, *Lecture Notes Comput. Sci.*, May 2007, pp. 773–782.

[27] S. Thomson, T. Narten, and T. Jinmei, IPv6 stateless address autoconfiguration, RFC 4862, Sep. 2007.

[28] T. Camp, J. Boleng, and V. Davies, "A survey of mobility models for ad hoc network research," *Wireless Commun. Mobile Comput.*, vol. 2, no. 5, pp. 483–502, Aug. 2002.

[29] V. Davies, "Evaluating mobility models within and ad hoc network," M.S. thesis, Dept. Math. Comput., Colorado School of Mines, Golden, CO, USA, 2000.

[30] M. S. Hossain and M. Atiquzzaman, "Cost analysis of mobility protocols," *Telecommun. Syst.*, vol. 52, no. 4, pp. 2271–2285, Apr. 2013.

[31] M. S. Hossain and M. Atiquzzaman, "Stochastic properties and application of city section mobility model," in *Proc. IEEE GLOBECOM*, 2009, pp. 1–6.

[32] S. Ryu, K. Lee, and Y. Mun, "Optimized fast handover scheme in mobile IPv6 networks to support mobile users for cloud computing," *J. Supercomput.*, vol. 59, no. 2, pp. 658–675, Feb. 2012.

[33] Y. -B. Lin, "Modeling techniques for large-scale PCS networks," *IEEE Commun. Mag.*, vol. 35, no. 2, pp. 102–107, Feb. 1997.

[34] C. Makaya and S. Pierre, "An analytical framework for performance evaluation of IPv6-based mobility management protocols," *IEEE Trans. Wireless Commun.*, vol. 7, no. 3, pp. 972–983, Mar. 2008.

[35] J. McNair, I. F. Akyildiz, and M. D. Bender, "An inter-system handoff technique for the IMT-2000 system," in *Proc. INFOCOM*, 2000, pp. 208–216.

[36] J. Xie and I. F. Akyldiz, "A novel distributed dynamic location management scheme for minimizing signaling costs in mobile IP," *IEEE Trans. Mobile Comput.*, vol. 1, no. 3, pp. 163–175, Jul.–Sep. 2002.

[37] N. Aschenbruck, R. Ernst, E. Gerhards-Padilla, and M. Schwamborn, "BonnMotion—A mobility scenario generation and analysis tool," in *Proc. SIMUTools*, Torremolinos, Spain, 2010, pp. 1–10.

[38] Seoul Metropolitan Government. Report on velocity of vehicles in Seoul 2010. [Online]. Available: http://traffic.seoul.go.kr/wp-content/themes/seoul_traffic/data/2010_3.pdf

[39] Seoul Expressway Traffic Control Center. Seoul Expressway Traffic Information. 2012. [Online]. Available: http://smartway.seoul.go.kr/english/index.html

[40] J. T. Park and S. M. Chun, "Fast mobility management for delay-sensitive applications in vehicular networks," *IEEE Commun. Lett.*, vol. 15, no. 1, pp. 31–33, Jan. 2011.

[41] S. Pack, J. Choi, T. Kwon, and Y. Choi, "Fast-handoff support in IEEE 802.11 wireless networks," *IEEE Commun. Surveys Tut.*, vol. 9, no. 1, pp. 2–12, 1st Quart., 2007.

[42] J. McNair, I. F. Akyildiz, and M. D. Bender, “Handoffs for real-time traffic in mobile IP version 6 networks,” in *Proc. IEEE GLOBECOM*, 2001, pp. 3463–3467.
[43] C. Fraleigh, S. Moon, B. Lyles, C. Cotton, M. Khan, D. Moll, R. Rockell, T. Seely, and C. Diot, “Packet-level traffic measurements from the Sprint IP backbone,” *IEEE Netw.*, vol. 17, no. 6, pp. 6–16, Nov./Dec. 2003.
[44] H. Soliman, C. Castelluccia, K. ElMalki, and L. Bellier, Hierarchical mobile IPv6 (HMIPv6) mobility management, RFC 5380, Oct. 2008.
[45] S. Gundavelli, K. Leung, V. Devarapalli, K. Chowdhury, and B. Patil, Proxy mobile IPv6, RFC 5213, Aug. 2008.
[46] J. H. Lee, T. Ernst, and N. Chilamkurti, “Performance analysis of PMIPv6 based network mobility for intelligent transportation systems,” *IEEE Trans. Veh. Technol.*, vol. 61, no. 1, pp. 74–85, Jan. 2012.
[47] S. Ryu, J.-W. Choi, and K.-J. Park, “A scheme improving fast PMIPv6-based network mobility by eliminating tunneling overload for ITS,” in *Proc. IEEE IV Symp.*, Jun. 2012, pp. 1–6.

Seonggeun Ryu received the B.S. degree in computer science from Yonsei University, Seoul, Korea, in 2002 and the M.S. and Ph.D. degrees from Soongsil University, Seoul, in 2006 and 2011, respectively.

From 2011 to 2013, he was a Postdoctoral Researcher with the Department of Information and Communication Engineering, Daegu Gyeongbuk Institute of Science and Technology, Daegu, Korea. He is currently with LG Electronics, Seoul, Korea. His research interests include analyzing, modeling, improving, and securing Internet-Protocol-based mobility management protocols for next-generation wireless networks and vehicular networks.

Kyung-Joon Park (S’01–M’05) received the B.S. and M.S. degrees in electrical engineering and the Ph.D. degree in electrical engineering and computer science from Seoul National University, Seoul, Korea.

From 2001 to 2002, he was a Visiting Graduate Student with the Department of Electrical and Computer Engineering, University of Illinois at Urbana-Champaign (UIUC), Urbana, IL, USA. From 2005 to 2006, he was a Senior Engineer with Samsung Electronics, Suwon, Korea. From 2006 to 2010, he was a Postdoctoral Research Associate with the Department of Computer Science, UIUC. He is currently an Assistant Professor with the Department of Information and Communication Engineering, Daegu Gyeongbuk Institute of Science and Technology, Daegu, Korea. His current research interests include modeling and analysis of cyber–physical systems and the design of medical-grade protocols for wireless healthcare systems.

Dr. Park is currently serving on the editorial boards of the *Wiley Transactions on Emerging Telecommunications Technologies*. He has served as a Lead Guest Editor for a special issue on cyber–physical systems in *Computer Communications*. He has also served as a program committee member of numerous international conferences on wireless networking. He received the Gold Prize at the Samsung InsideEdge Thesis Competition.

Ji-Woong Choi (S’00–M’04–SM’09) received the B.S., M.S., and Ph.D. degrees in electrical engineering from Seoul National University (SNU), Seoul, Korea, in 1998, 2000, and 2004, respectively.

From 2004 to 2005, he was a Postdoctoral Researcher with the Interuniversity Semiconductor Center, SNU. From 2005 to 2007, he was with the Department of Electrical Engineering, Stanford University, Stanford, CA, USA, as a Postdoctoral Visiting Scholar. From 2006 to 2007, he also worked as a Consultant with GCT Semiconductor, San Jose, CA, USA, on the development of mobile TV receivers. From 2007 to October 2010, he was with Marvell Semiconductor, Santa Clara, CA, USA, as a Staff Systems Engineer for next-generation wireless communication systems, including Worldwide Interoperability for Microwave Access and Long-Term Evolution. Since October 2010, he has been with the Department of Information and Communication Engineering, Daegu Gyeongbuk Institute of Science and Technology, Daegu, Korea, as an Assistant Professor. His research interests include wireless communication theory, signal processing, biomedical communication applications, and brain–machine interfaces.

Dr. Choi received the Silver Award at the Samsung Humantech Paper Contest in February 2005 and the IT National Scholarship from the Korean Ministry of Information and Communication in October 2005.